Phosphatase of Regenerative Liver-2 mediates cellular metabolic reprogramming in breast cancer

Tzvetena Hristova
Department of Biochemistry
McGill University
Montreal, Quebec, Canada

July 2018

A thesis submitted to McGill University in partial fulfillment of the requirements of the degree of Master of Science

TABLE OF CONTENTS

LIST OF FIGURES

ABSTRACT

The three Phosphatase of Regenerative Liver (PRL-1, -2, -3 or *PTP4A1, 2, 3*) enzymes represent a group of protein tyrosine phosphatases that has been implicated in a number of diseases, and largely studied in the context of cancer metastasis. However, little is known about their physiological function. We previously showed that PRL-2 plays a key role in breast cancer progression by regulating intracellular magnesium levels. Characterization of the PRL-2 knockout mouse indicates that PRL-2 expression is both gender and circadian rhythm dependent. PRL-2 modulation leads to altered magnesium homeostasis resulting in changes in energy metabolism. This is of interest since breast cancer cells undergo a metabolic switch to aerobic glycolysis, known as the Warburg effect. In addition, we have shown that ATP citrate lyase expression is decreased upon loss of PRL-2, suggesting a potential role of the PRLs in fatty acid synthesis. We are using an inducible shRNA model to knock down PRL members and study their role in breast cancer metabolism *in vitro*. Results show that loss of PRL-2 in breast cancer induces a metabolic stress, due to lower ATP levels within the cells caused by impaired glucose and glutamine metabolism. Furthermore, the fatty acid synthesis pathway is inhibited, and cholesterol accumulation is favoured upon PRL-2 loss. Defining the metabolic role of this phosphatase family would not only provide a greater understanding of the physiological processes governed by these unique PTPs but could also contribute insight into potential pathological mechanisms.

RÉSUMÉ

Les trois *Phosphatase of Regenerative Liver* (PRL-1, -2, -3 ou *PTP4A1, 2, 3*) représentent un groupe de protéines tyrosine phosphatases impliquées dans un certain nombre de maladies et largement étudiées dans le contexte des métastases cancéreuses. Cependant, peu d'information est disponible sur leur fonction physiologique. Précédemment, notre groupe a démontré que PRL-2 joue un rôle clé dans la progression du cancer du sein en régulant les niveaux de magnésium intracellulaire. La caractérisation de la souris knock-out PRL-2 indique que l'expression de PRL-2 dépend à la fois du sexe et du rythme circadien. La modulation de PRL-2 entraîne une altération de l'homéostasie du magnésium causant des changements dans le métabolisme énergétique. Ceci est intéressant, car les cellules cancéreuses du sein subissent un changement métabolique vers la glycolyse aérobie, connu sous le nom d'effet Warburg. En outre, nous avons montré que l'expression de l'ATP citrate lyase est diminuée lors de la perte de PRL-2, suggérant un rôle potentiel des PRL dans la synthèse des acides gras. Nous utilisons un modèle d'ARNsh inductible pour abattre les membres du PRL et étudier leur rôle dans le métabolisme du cancer du sein *in vitro*. Les résultats démontrent que la perte de PRL-2 dans le cancer du sein induit un stress métabolique, en raison de la diminution des taux d'ATP dans les cellules causée par une altération du métabolisme du glucose et de la glutamine. En outre, la voie de synthèse des acides gras est inhibée, et l'accumulation de cholestérol est favorisée lors de la perte de PRL-2. La définition du rôle métabolique de cette famille de phosphatases permettrait non seulement de mieux comprendre les processus physiologiques régis par ces PTP uniques, mais pourrait également contribuer à la compréhension de mécanismes pathologiques potentiels.

ACKNOWLEDGEMENTS

First and foremost, I am grateful to my supervisor, Dr. Michel L. Tremblay, for his guidance and mentoring, without which this project would not have been possible. Many thanks to my research committee members, Dr. William Pastor and Dr. Peter Siegel, who provided valuable advice. I would like to especially thank Dr. Serge Hardy who helped me immensely push this project forward. Huge thanks to Elie Kostantin who encouraged me and thought me new techniques when needed. I would like to give thanks to Teri Hatzihristidis for patiently teaching me lab techniques when I first got to the lab, she is the reason I decided to pursue graduate studies. I am also very grateful to Valérie Vinette who thought me how to perform and analyze Seahorse assays. I would also like to thank all other lab members who helped me throughout the way and who made my Master's so enjoyable. The McGill Metabolic Core Facility was instrumental in providing technical advice as well as the tools necessary to perform the experiments presented in this thesis.

Finally, this work was made possible by the financial support from the Canadian Institutes of Health Research (CIHR), the Biochemistry Graduate Research Enhancement and Travel Award (GREAT) and the Canderel Travel Award.

LIST OF ABBREVIATIONS

ACC1 or *ACACA*	Acetyl-CoA carboxylase 1
ACLY	ATP citrate lyase
ADP	Adenosine diphosphate
AKT	Protein kinase B
AMP	Adenosine monophosphate
AMPK	AMP-activated protein kinase
ATP	Adenosine triphosphate
CNNM	Cyclin-M
CPT1	Carnitine palmitoyl-CoA transferase 1
DSPs	Dual-specific PTPs
ECAR	Extracellular Acidification Rate
ERα	Estrogen receptor α
ERRα	Estrogen-related receptor α
ETC	Electron transport chain
FASN	Fatty acid synthase
FH	Fumarate hydratase
GLS	Phosphate-dependent glutaminase
IDH	Isocitrate dehydrogenase
KD	Knockdown
KO	Knockout
Mg^{2+}	Magnesium

OCR	Oxygen Consumption Rate
PGC1α	Peroxisome proliferator-activated receptor gamma coactivator 1-alpha
PPARα	Peroxisome proliferator-activated receptor alpha
PRL-1 or *PTP4A1*	Phosphatase of Regenerative Liver 1
PRL-2 or *PTP4A2*	Phosphatase of Regenerative Liver 2
PRL-3 or *PTP4A3*	Phosphatase of Regenerative Liver 3
PTPs	protein tyrosine phosphatases
RPTPs	Transmembrane receptor like PTPs
SDH	Succinate dehydrogenase
SREBP1c	Sterol-regulatory-element-binding protein 1c
TCA	Tricarboxylic acid
UCP1	Uncoupling protein 1
WT	Wild type
XF	Seahorse Extracellular Flux

INTRODUCTION

1. Protein Tyrosine Phosphatases

Protein phosphorylation is a key post-translation modification leading to the addition of a phosphate molecule to an amino acid residue on a protein inducing a conformational change of the protein and altering its biological properties [1]. This phosphorylation event is tightly controlled by two enzyme families, the protein kinases, which phosphorylate, and the protein phosphatases, which dephosphorylate [2]. Evolutionarily, the protein phosphatase family has evolved into multiple distinct sub-families of phosphatases having different mechanisms of action [3]. The serine/threonine phosphatase super family dephosphorylates serine or threonine residues specifically, whereas the protein tyrosine phosphatases (PTPs) superfamily is well known to remove phosphates from tyrosine residues, leading to the regulation of multiple physiological processes in the cell, such as growth, metabolism and differentiation [3, 4].

The human genome encodes 107 PTP genes, which can be divided into four PTP families based on the amino acid sequences of their catalytic domains [5]. Class I, II and III PTPs are cysteine-based, they depend on a cysteine residue for their catalytic activities, whereas class IV PTPs depend on an aspartic acid residue and a cation for catalytic activity [5]. Class I PTPs is the largest family and is composed of the “dual-specific” PTPs (DSPs) and the “classical” PTPs, which are further subdivided into the transmembrane receptor like PTPs (RPTPs) and the intracellular nonreceptor PTPs [5]. RPTPs regulate signalling through ligands and are often involved in cell-cell contact as they have cell-adhesion properties [6]. The intracellular PTPs control activity through sequences flanking the catalytic sites allowing for direct interactions with the active site or through substrate specificity [7]. The DSPs are a heterogenous group, less well conserved

than the classical PTPs, allowing to interact with phosphoserine/phosphothreonine residues as well as phosphotyrosine residues in their active sites [8].

All PTP members use a similar catalytic mechanism, involving the $HC(X)_5R$ motif containing the essential cysteine group which will recognize the targeted phosphate [4]. Catalysis is a two-step process, where there will first be the formation of the cysteinyl-phosphate intermediate which will then be hydrolyzed, usually mediated by a glutamine residue [4]. Finally, oxidation at the cysteine residue of the active site will end its nucleophilic activity, inhibiting at the same time the PTP activity [4].

As PTPs have been shown to have tumour-suppressive functions, as well as oncogenic activity in different cancer types, these enzymes have become very interesting in the cancer field, and are now thought to be interesting therapeutic targets [9, 10].

2. Phosphatase of Regenerative Liver

The three **P**hosphatase of **R**egenerative **L**iver (PRL-1, -2, -3 or *PTP4A1, 2, 3*) enzymes represent a group of protein tyrosine phosphatases that, like most PTPs, possess a conserved $V/IHCX_5R$ motif [11]. However, the PRL family, unlike other PTPs, also possesses a prenylation motif, guiding their localization to the endosomal compartment and plasma membrane [12-14]. The PRLs are dual-specificity phosphatases, with a potential action on both tyrosine and serine/threonine residues [15]. In humans, PRL-1 and PRL-2 are ubiquitously expressed, whereas PRL-3 is mainly found in the heart, skeletal muscle and prostate [16, 17]. To date, no specific PRL substrate has been clearly identified [18].

The PRLs have been largely studied in the context of cancer metastasis and have gained great attention as potential targets for cancer treatment. PRL-3 has been strongly associated with triple-negative breast cancer and has correlated with both poorer survival and metastasis [19]. Similarly, *in vitro* PRL-3 knockdown reduced cell proliferation and migration in multiple cancer cell types such as melanoma, gastric, ovarian and lung cancers [20-25]. Parallel observations have been shown in cervical and gastric cancers, where PRL-1 was reported to be overexpressed [26, 27]. Also, PRL-2 expression was higher in primary breast tumours compared to normal tissue, as well as higher in metastatic lymph nodes compared to primary tumours [21]. It has also been shown that PRL-2 is a target of estrogen receptor α (ERα) and estrogen-related receptor α (ERRα) in MCF7 breast cancer cell lines [28]. PRL-2 overexpression in a breast cancer transgenic mouse model increased tumour progression and lead to the discovery of a direct interaction between the PRLs and the cyclin-M (CNNM) magnesium transporter family, composed of CNNM1-4 [21, 29]. The CNNMs have also been shown to interact with AMP, ADP, ATP and Mg-ATP contributing to their Mg sensing/transport capacities [30-33]. It was also shown in breast cancer that upon Mg^{2+} depletion, PRL-1 and PRL-2 protein levels were upregulated also leading to improved association with CNNM3, causing increased intracellular magnesium levels through a proposed influx mechanism [29].

As most publications on the PRL family are focused on cancer, little is known about the PRLs physiological function. PRL-1 knockout (KO) mice grow normally, while PRL-2 KO males display mild impaired reproductive abilities, which has been attributed to the functional redundancy of PRL-1 and PRL-2 in mice [34, 35]. However, there were no viable PRL-1/PRL-2 double KO embryos passed E9.5 days, suggesting that expression of either PRL-1 or PRL-2 alone is

sufficient for survival [34]. Characterization of the PRL-2 knockout mouse indicates that PRL-2 expression is both gender and circadian rhythm dependent [36]. In addition, ATP citrate lyase (ACLY) gene expression is decreased upon loss of PRL-2, suggesting a potential role of the PRLs in fatty acid synthesis [36]. Furthermore, accumulation of certain metabolites in the tricarboxylic acid (TCA) cycle, such as citrate, α-ketoglutarate, succinate, fumarate and malate have also been shown in the PRL-2 KO mice compared to wild type (WT) mice [36]. Finally, differences in uncoupled respiration have also been reported, where higher uncoupled respiration as well as higher expression of uncoupling protein 1 (UCP1) have been reported in PRL-2 KO mice [36].

4. Magnesium Homeostasis

Magnesium is the second most abundant and essential intracellular cation regulating numerous cellular functions and enzymes involved in metabolic pathways [19, 37]. Studies have shown that the total Mg^{2+} concentration present in most mammalian cells ranges between 17mM and 20mM, whereas free Mg^{2+} concentrations have been reported to be between 0.8mM and 1.2mM [37-40]. Furthermore, rapid Mg^{2+} fluxes across the plasma membrane, either through channels or carriers, have been reported in response to metabolic or hormonal stresses [41-44]. Interestingly, free Mg^{2+} levels in the cell hardly fluctuate, reporting a rapid Mg^{2+} buffering capacity of the cells [45, 46].

Magnesium homeostasis has also been linked to glucose metabolism [47, 48]. In liver cells, it was shown that certain hormones leading to Mg^{2+} release from the cell concomitantly lead to glucose extrusion [49]. Furthermore, enzymes involved in glucose metabolism, such as

hexokinase, phosphofructokinase, enolase, pyruvate kinase and many more, are activated under low Mg^{2+} conditions and inhibited when Mg^{2+} levels are high [47, 48].

Further studies have shown Mg^{2+} to be important in protein synthesis and ATP production as these processes are impeded upon lower total Mg^{2+} levels in the cell [50]. In fact, ATP has been reported to be the major buffering agent of Mg^{2+} in the cell, such that upon considerable ATP utilization, increase in free Mg^{2+} in the cell is reported, followed by Mg^{2+} extrusion [51, 52]. Thus, it seems that Mg^{2+} homeostasis is closely linked to cell metabolism either through glucose metabolism, ATP or other mechanisms.

5. Glucose Metabolism

Glucose is essential for ATP production within the cell [53]. To produce ATP, glucose must first be transformed into pyruvate through glycolysis, which occurs in the cytoplasm [54]. Pyruvate is then transformed into acetyl-CoA once in the mitochondria, where it will go through the TCA cycle and the electron transport chain (ETC) to produce larger ATP amounts [53].

The glycolytic pathway involves multiple tightly regulated enzymes producing intermediates which can be used for other purposes than energy within the cell, such as production of fat or amino acids [55]. One enzyme of interest is hexokinase, which phosphorylates glucose to glucose-6-phosphate, requiring ATP and Mg^{2+} to do so [55]. Hexokinase is activated by changes in AMP/ADP ratios and is inhibited by elevated levels of glucose-6-phosphate [56, 57]. Two other enzymes are crucial in this pathway, phosphofructokinase and pyruvate kinase, both of which are also activated by AMP/ADP ratios and other allosteric regulators [56]. Elevated levels of ATP inhibit both phosphofructokinase and pyruvate kinase, where elevated citrate levels are

only inhibitory to phosphofructokinase, and elevated acetyl-CoA levels predominantly inhibit pyruvate kinase [57]. Glycolysis alone produces only a total of two ATP molecules per glucose molecule, which is why mitochondrial function and TCA cycle regulation is very important to supply larger amounts of ATP [53, 58]. The TCA cycle also produces certain metabolic intermediates which will be funneled into other anabolic pathways leading to lipid, proteins and nucleic acid production [59]. Some of these intermediates are citrate, α-ketoglutarate and oxaloacetate which are used mainly in *de novo* lipid synthesis as well as *de novo* nucleic acid synthesis [53].

In cancer, cells rely heavily on glycolysis as their main energy producing pathway rather than mitochondrial oxidative phosphorylation [60]. Indeed, a larger glucose uptake as well as larger glycolytic rates have been observed in many cancer cell types [55, 61]. Even under the presence of oxygen, cells will undergo aerobic glycolysis, also known as the Warburg effect, which leads to the production of lactate from pyruvate [61]. This process is preferred as it allows for rapid energy production leading to rapid proliferation and intermediate production allowing for quick macromolecule synthesis [61, 62]. Although the TCA cycle does not seem to be required in cancer cell energetics, it must be conserved to avoid cell death [59]. Further studies have shown that mutations in TCA cycle enzymes, such as isocitrate dehydrogenase (IDH), succinate dehydrogenase (SDH) and fumarate hydratase (FH), may lead to accumulations in certain intermediates that can potentially lead to tumour progression [63-65].

Nowadays, Seahorse Extracellular Flux (XF) Analyzers are widely used to study cell metabolism by measuring glycolytic and cellular respiration rates [66]. Extracellular Acidification Rate (ECAR) plate-based experiments are performed to measure the rate of medium acidification in

order to report glucose oxidation rates [66]. This produces an ECAR profile from which the glycolytic rate, glycolytic capacity and glycolytic reserve rates can be extrapolated [66]. Similarly, Oxygen Consumption Rate (OCR) plate-based experiments allow to measure cellular respiration and mitochondrial integrity [66]. OCR assays measure oxygen content within the medium producing a OCR profile from which basal respiration, ATP-linked respiration, uncoupled respiration, maximal respiration and reserve capacity, also known as spare respiratory capacity, can be extrapolated [66].

6. Lipid Metabolism

Lipids provide a great energetic source in the body such that lipid storage becomes a crucial event in providing energy and sustain metabolism under stressful conditions such as starvation [67]. Many cancer cells will increase their lipid synthesis pathways in order to sustain and increase cellular activity in harsh conditions [68]. Three major enzymes are involved in the production of fatty acids and phospholipids: ATP citrate lyase (ACLY), Acetyl-CoA carboxylase 1 (ACC1) and fatty acid synthase (FASN) [69-71]. Tight regulation of those three enzymes allows the cells to respond to different stimuli and either activate lipid synthesis or inhibit it, thus promoting lipid oxidation and production of energy [69-71].

ACLY is a critical cytosolic enzyme which links glucose metabolism to lipid production by producing acetyl-CoA from cytosolic citrate coming from the mitochondria [69]. This acetyl-CoA is then used by two distinct pathways, either for fatty acid synthesis through ACC1 or for cholesterol synthesis [69]. Studies have shown that inhibition of ACLY decrease both fatty acid and cholesterol synthesis [69]. Furthermore, acetyl-CoA production by ACLY can be used for

histone acetylation reactions thus controlling gene expression [72, 73]. ACLY activation and expression can be increased through insulin stimulation and its activation is mediated by protein kinase B (AKT) phosphorylation at serine 454 [74, 75].

ACC1, encoded by the *ACACA* gene, is the rate determining step in this pathway and is crucial in transforming acetyl-CoA into malonyl-CoA, which is a strong inhibitor of beta oxidation through the inhibition of carnitine palmitoyl-CoA transferase 1 (CPT1) [70, 76, 77]. ACC1 expression is tightly regulated by a multitude of factors. Indeed, *ACACA* gene expression is under the control of three promoters which respond differently to different stimuli such as glucose, thyroid hormone, insulin, catabolic hormones and leptin [78-81]. Generally, ACC1 will be inhibited under starvation conditions and will be activated in opposite circumstances, when nutrients are readily available to be transformed and stored [82]. Furthermore, sterol-regulatory-element-binding protein 1c (SREBP1c) is a major transcriptional activator playing a key role in regulating not only *ACACA* expression but all other major enzymes involved in lipogenesis [83]. ACC1 is also regulated allosterically, being activated by the presence of insulin, citrate and glutamate and inhibited by high levels of malonyl CoA and fatty acyl-CoA esters [84-87]. Furthermore, ACC1 is inhibited by its phosphorylation on several serine residues upon AMP-activated protein kinase (AMPK) activation [88].

AMPK is an energy sensor that is activated upon phosphorylation on threonine-172 in response to lower ATP levels in the cell, which increase the AMP/ATP ratio [89]. When AMPK is activated, anabolic processes and cell proliferation are stopped, and catabolic processes are activated in order to provide enough fuel to keep the cell alive [89]. AMPK is only inactive when the cell has

enough nutrients for proper metabolic processes [90]. Thus, AMPK and ACC can be used as markers to assess energetic stress in the cells.

FASN has for function to produce palmitate from acetyl-CoA and malonyl-CoA [76]. Its expression is regulated by SREBP1c transcription factor and through insulin signalling [76]. FASN has been identified as an oncogene and is upregulated in breast cancer [91].

7. Glutamine metabolism

Glutamine is a non-essential amino acid and one of the most abundant ones in the body [92]. It is involved in many cellular processes such as energy homeostasis, protein synthesis, nucleic acid synthesis and it is a nitrogen and carbon donor to the TCA cycle [93]. Glutamine is important for glutathione synthesis, which is part of the cell's defense mechanism against oxidative stress [94]. Furthermore, glutamine is used as a fuel to allow rapid cell proliferation when required and is a key player in gluconeogenesis [93].

In cancer, cells have developed mechanisms leading to greater glutamine uptake and metabolism [94, 95]. In cancer cells, glutamine is an important source of energy for rapid cell proliferation and enhanced growth [94]. Glutamine is transformed into glutamate by phosphate-dependent glutaminase (GLS), which in turn will produce α-ketoglutarate through IDH function [96]. α-Ketoglutarate can then be either channeled through the TCA cycle to eventually produce aspartate, or it can be transformed into isocitrate and then citrate, which will be used by ACLY for lipid synthesis [97, 98].

OBJECTIVES

It is well established that the PRL family is involved in breast cancer progression and has oncogenic properties, but no mechanism of action has yet been described [21, 29]. Recent studies have linked PRL-2 to the CNNM family, which modulates Mg^{2+} homeostasis [30-33]. PRL-2 has also been linked to fatty acid synthesis and TCA cycle intermediate accumulation [36]. These taken together have suggested a potential role of action of PRL-2 in metabolism. This study's overall aim was to establish a role of PRL-2 in breast cancer metabolism, as well as to provide new insight on its mechanism of action within the metabolic pathways. Defining the metabolic role of this phosphatase family would not only provide a greater understanding of the physiological processes governed by these unique PTPs, but could also contribute insight into potential pathological mechanisms, leading to better breast cancer therapeutics.

MATERIALS AND METHODS

1. Cell Culture

MCF7 and MDA-MB-231 human cell lines were maintained in culture in complete DMEM media (Gibco) supplemented with 10% Fetal Bovine Serum (FBS) (Gibco) and 1X Gentamycin (Wisent). All cell lines were cultured at 37°C in 5% CO_2 incubator. The inducible shRNA MCF7 and MDA-MB-231 models were induced for 48 hours by addition of 1X doxycycline (dox) (Sigma) for a final concentration of 1μg/mL dox, prior to any other cell treatments. MCF7 and MDA-MB-231 cell starvation was performed using complete DMEM media (Gibco) supplemented with 1X Gentamycin (Wisent) only. Insulin stimulation experiments required addition of 10μg/mL of insulin (Wisent) in the media used. Glucose treatment experiments required DMEM media without glucose (Gibco) supplemented with 10% FBS (Gibco), 1X Gentamycin (Wisent) and glucose for a final concentration of 5mM, low glucose conditions, and 25mM, high glucose conditions. Experiments involving different Mg^{2+} concentration conditions required DMEM free of Mg^{2+} and Ca^{2+} (Multicell) supplemented with 1X GlutaMAX (Gibco), calcium chloride (Sigma), 10% dialyzed FBS (Life Technologies, Thermo Fisher Scientific) and the appropriate amount of magnesium sulfate (Sigma) to obtain the desired Mg^{2+} concentration in the media.

2. Generation of inducible shRNA model

Stable reverse tetracycline-controlled transactivator (rtTA) MDA-MB-231 and MCF7 cells were generated using CRISPR/Cas9 technology by targeting rtTA in the AAVS1 safe harbor human locus. sgRNA targeting the AAVS1 locus was cloned into pSpCas9(BB)-2A-GFP (PX458) (Addgene plasmid no. 48138). DNA fragment consisting of the CAG promoter located in front of an rtTA-

T2A-Fluc transgene was generated by overlapping PCR and cloned into the AgeI/EcoRI sites of pZDonor-AAVS1 Puromycin targeting vector (Sigma). This targeting vector was then co-transfected along with the CRISPR/Cas9 AAVS1 sgRNA construct in MDA-MB-231 and MCF7 using Fugene HD (Roche) and clones were selected for puromycin resistance (5 ug/ml). The newly generated rtTA MDA-MB-231 and MCF7 cells were then infected with two individual shRNAs targeting PRL-2 and a scramble control, which were cloned using gateway system (Invitrogen) into the lentiviral vector pLentiCMVTRE3G_Neo_Dest (Addgene plasmid no. 27566). Cells were selected with G418 (800 ug/ml) and used as a pool for the various assays described in this study. shRNAs expression was induced using 1 ug/ml of doxycycline (Sigma).

3. Western Blot

Cell lysis was performed to obtain whole cell extracts (WCE) by first preparing a cell lysis buffer containing modified RIPA buffer (mRIPA) supplemented with 1X protease inhibitor (Roche), 2mM sodium orthovanadate and 5mM sodium fluoride. To each well of a 6 well plate, 50μL of lysis buffer was added, the adherent cells were scraped and transferred to a 1.5mL Eppendorf tubes. WCE were incubated on ice for 15 minutes after which cell debris were pelleted by centrifugation at maximum speed for 15 minutes at 4°C. Protein concentration of WCE was measured using Pierce BCA Protein Assay kit (Thermo Fisher Scientific). 15-20μg of protein were diluted in mRIPA and 4X Laemmeli buffer and were then boiled for 5 minutes at 100°C. Protein lysates were resolved by 8%, 10% or 12% SDS-PAGE followed by 60 minutes semi-dry transfers (for 12% gels) or overnight wet transfers (for 8% and 10% gels) performed on PVDF membranes. Western blot analysis was performed using the following antibodies: 1:1000 PRL-

1/2 (Millipore), 1:1000 pACC (Cell Signalling), 1:2000 ACC (Cell Signalling), 1:2000 pACLY (Cell Signalling), 1:2000 ACLY (Cell Signalling), 1:1000 pAKT (Cell Signalling), 1:2000 AKT (Cell Signalling), 1:2000 pAMPK (Cell Signalling), 1:2000 AMPK (Cell Signalling), 1:2000 pIR (Biosource), 1:2000 IR (Cell Signalling), 1:1000 FASN (Cell Signalling), 1:2000 Actin (Sigma), and 1:10 000 Calnexin (Gift from Dr. J. Bergeron). Horse radish peroxidase-coupled secondary antibodies and Western Lightning ECL Pro (PerkinElmer) were used to visualize protein levels on a ChemiDoc XRS+ Imager (BioRad).

4. Acetyl-CoA measurements

Cells were seeded in 15cm plates (n=4) and were treated as mentioned above. After 48h dox induction, cells were washed with cold 1XPBS before trypsin (Wisent) treatment and 5 minutes incubation in a 37°C in 5% CO_2 incubator. Cells were counted and $2x10^6$ cells per replicate were transferred into a 1.5mL sterile Eppendorf and resuspended in 250µL of Acetyl CoA Assay Buffer (abcam). Samples were sonicated for 10 minutes at high intensity, 30sec on, 30sec off. After centrifugation at maximal speed at 4°C for 10 minutes, deproteinization was performed by using 3kDa spin filters (Millipore). Acetyl-CoA levels were measured in duplicates using the final supernatant obtained and following PicoProbe Acetyl CoA Assay Kit (abcam) per manufacturer's instructions.

5. Cholesterol Assay

Cells were seeded in tissue culture treated 12 well plates (Costar), 5 replicates per cell type were used for cholesterol measurements and 5 replicates from the same plate were used to

count cells for normalization purposes using a TC10 cell counter (BioRad). At 0h dox induction, $1x10^5$ cells were seeded per well and were treated as mentioned in the "Cell Culture" section above. After 48h dox induction, the cells were washed with 1XPBS and were frozen at -80°C. Frozen cells were scrapped with a cell scraper and the 1X Reaction Buffer provided with the kit (Invitrogen). Lysates were transferred to 1.5mL Eppendorf tubes and were sonicated for 10 minutes at high intensity, 30sec on and 30sec off. Sonicated cell lysates were used to measure cholesterol levels using Amplex Red Cholesterol Assay Kit (Invitrogen) as per manufacturer's instructions.

6. ATP Level Measurements

Cells were seeded in two cell culture treated flat bottom 96 well plates (Falcon). Replicates (n=5 or n=6) were treated as mentioned above in "Cell Culture" section. $5x10^3$ cells were seeded per well. One 96 well plate was used for the ATP analysis, whereas the other was used for CyQuant Proliferation Assay (Invitrogen) analysis to determine the total DNA content for normalization purposes. Both plates were treated in the exact same manner, where after 48h dox induction, the media was flicked off from the plate and cells were frozen at -80°C. ATP levels were measured using CellTiter-Glo® Luminescence Cell Viability Assay (Promega) as per manufacturer's instructions. CyQuant Proliferation Assay (Invitrogen) was performed as per manufacturer's instructions.

7. Metabolite measurements

MDA-MB-231 cells were seeded in cell culture treated 6 well plates (Costar) and were treated as described in the "Cell Culture" section above. A media change was performed at approximately 30h dox induction to enrich the media with 1X GlutaMAX (Gibco) for 18hours. At 48h dox, 1mL of media per well was collected and transferred to a sterile 1.5mL Eppendorf tube. Samples were centrifuged at maximal speed at 4°C for 10 minutes before measuring glucose, glutamine, lactate and glutamate levels remaining in the media using a BioProfile 400 Analyzer (Nova Biomedical). Analyte concentrations obtained were normalized to total cell number. Cell number was calculated using a TC10 cell counter (BioRad).

8. Seahorse assay

MDA-MB-231 cells were pretreated with dox for 48h. $1x10^4$ cells were plated per well in XF96 cell culture microplate (Seahorse bioscience). After overnight incubation, cell media was replaced with Seahorse assay media and the cells were incubated for 1h in a 0% CO_2 incubator. Half of the plate was used to measure Extracellular acidification rate (ECAR) and the other half was used to measure oxygen consumption rate (OCR) following manufacturer's instructions (Agilent). To perform ECAR assay, 10mM glucose, 1.5μM oligomycin, 100mM 2-deoxyglucose was added to the cells. To perform OCR assay 1.5μM oligomycin, 1.0μM FCCP and 1.0μM rotenone was added to the cells. ECAR and OCR values were normalized to total DNA content by performing a CyQuant Proliferation Assay (Invitrogen) following manufacturer's instructions.

9. Cell proliferation assay

The IncuCyte ZOOM system (Essen bioscience) was used to assess cell proliferation. $5x10^3$ MDA-MB-231 inducible shSCR, $shPTP4A2_{(2)}$ and $shPTP4A2_{(3)}$ cells were seeded per well in a cell culture treated flat bottom 96 well plate with addition of 1µg/mL dox. The cells were directly transferred to the IncuCyte ZOOM (Essen bioscience). Cell confluency was measured every 8 hours for a total 160 hours. The IncuCyte ZOOM integrated software analyzes all images, 4 images per well, taken over time to produce a proliferation curve for each cell type. 5 replicates of each cell type were seeded. Proliferation curves can then be compared between the samples to determine if differences in proliferation occur.

10. Statistical analysis

Statistical analysis was performed using GraphPad Prism® Version 7.0. One-way ANOVA statistical analysis was performed where applicable.

RESULTS

As there is strong evidence that PRL2 plays an important role in breast cancer progression, breast cancer human cell lines, MDA-MB-231 and MCF7, were chosen for this study [21, 28, 29]. Furthermore, PRL2 has been linked to ACLY gene expression, to uncoupled respiration and to TCA cycle intermediate levels under physiological conditions in the mouse, but no specific mechanism has been found to account for these effects [36]. The following results will further demonstrate a role of PRL-2 in breast cancer metabolism specifically, through the study of fatty acid synthesis, glycolysis and mitochondrial function.

1. MCF7 and MDA-MB-231 respond to insulin and express PRL-1 and PRL-2

PRL-2 has recently been linked to ACLY, which in turn links glucose metabolism to lipid synthesis [36]. Thus, studying ACLY activity in breast cancer while modulating PRL-2 expression was the first objective of this study. However, as ACLY activity is regulated through its phosphorylation upon insulin signaling, it was necessary to first assess MCF7 and MDA-MB-231 human cell lines' responsiveness to insulin stimulation [74, 75]. This was done through western blot, which also allowed to confirm PRL-1 and PRL-2 levels in those breast cancer cell lines.

Human breast cancer cell lines MCF7 and MDA-MB-231 were chosen for this study as strong PRL-1 and PRL-2 expression has previously been reported in those cell lines by our group [21]. Furthermore, MCF7 is estrogen-dependent and MDA-MB-231 is estrogen-independent, which allows to assess if estrogen has an effect on the role of PRL-2 in breast cancer metabolism [21]. As shown in figure 1, both MCF7 and MDA-MB-231 cell lines express the phosphorylated insulin receptor (pIR) upon insulin stimulation, which is not seen without the presence of insulin in the

media. Further insulin response is validated by the phosphorylation of AKT (pAKT) which then phosphorylates and activates ACLY [74, 75]. Furthermore, both MCF7 and MDA-MB-231 cell lines strongly express PRL-2. Expression of PRL-1 can also be seen in both cell lines. Thus, MCF7 and MDA-MB-231 cell lines seem to be ideal tools to study PRL-2 function in lipid metabolism.

2. Generation of an inducible shPTP4A2 model in MCF7 and MDA-MB-231 human cell lines.

As MCF7 and MDA-MB-231 cell lines were determined to be proper tools for this study, an inducible shPTP4A2 knock down (KD) model was generated (Figure 2 A). An inducible model was preferred in order to avoid metabolic adaptation of the cells upon PRL-2 KD, allowing to properly study the metabolic effect of PRL-2 in breast cancer. Two different shRNA for PRL-2 targeting were used, labeled shPTP4A2$_{(2)}$ and shPTP4A2$_{(3)}$. Through western blot analysis, it was determined that 48 hours doxycycline induction was optimal and lead to the greatest knockdown effect (Figure 2 B and C). As shown in Figure 2 C, MCF7 shPTP4A2$_{(3)}$ cells show only 40% KD efficiency, whereas the shPTP4A2$_{(2)}$ did not seem to work. Thus, further experiments in the MCF7 inducible model will be performed using only the shSCR and shPTP4A2$_{(3)}$ cell lines. On the other hand, the knockdown seems to be quite efficient in the MDA-MB-231 cell lines for both shPTP4A2s, where shPTP4A2$_{(2)}$ shows a 60% decrease and shPTP4A2$_{(3)}$ shows a 75% decrease in PRL-2 protein levels, thus both biological replicates will be used for further studies and will be compared to shSCR (Figure 2 B). Furthermore, as it was previously reported, upon PRL-2 knockdown there is a compensation by PRL-1, where PRL-1 protein levels increase upon PRL-2 loss [34, 35]. Also, PRL-1 compensation seems very strong in MDA-MB-231 cell lines but

less so in the MCF7, as the MCF7 cells already express high levels of PRL-1 when compared to PRL-2 levels. MDA-MB-231 cell lines express much less PRL-1 when compared to PRL-2 protein levels.

3. PRL-2 KD leads to the activation of ACLY and inhibition of ACC in breast cancer.

To assess the role of PRL-2 in the lipid synthesis pathway, PRL-2 deficient MDA-MB-231 and MCF7 cells, as shown in figure 2, were stimulated with insulin and western blotting was performed. Figure 3 A shows an upregulation of pAKT which leads to an upregulation of pACLY in the PRL-2 KD MCF7 cells upon insulin stimulation. Furthermore, there is higher AMPK phosphorylation in the PRL-2 KD MCF7 cells leading to a higher expression of pACC as well (Figure 3 A). However, FASN does not seem to be affected by PRL-2, as there is no change in protein levels that can be seen (Figure 3 A). This is also recapitulated in the MDA-MB-231 inducible cell lines, Figure 3 B, where high ACC phosphorylation is seen and seems to be PRL-2 dependent, as shPTP4A2$_{(2)}$ expresses more PRL-2 and has lower pACC compared to shPTP4A2$_{(3)}$, which expresses less PRL-2 but has higher pACC levels. In Figure 3 B, ACC levels also seem to be increased, however this increase is not always consistent when repeating the experiment, whereas pACC levels are always elevated. Furthermore, qPCR analysis (data not shown) does not show elevated gene expression levels of ACC upon PRL-2 KD. Thus, further experiments must be performed in order to fully understand the effect of PRL-2 KD on ACC. An effect on pAKT and pACLY can also be seen, especially at 20 minutes, but much less striking than in the MCF7 inducible cell line. The insulin stimulation effect can be confirmed in both Figure 3 A and B by the expression of pIR in the insulin stimulated samples.

As the MDA-MB-231 inducible model has the best knockdown efficiency, further studies will be performed with these cells only. Furthermore, in Figure 3 B, it can be seen that at 0h timepoint, which is equivalent to 24hours starvation, the effect on pACC is strongest, as the cells are under metabolic and energetic stress.

4. Knocking down PRL-2 induces metabolic stress in breast cancer.

As shown in Figure 3 B, pACC levels in MDA-MB-231 inducible model are highest in the knockdown cells after 24 hours starvation. Thus, it was hypothesized that the loss of PRL-2 expression in breast cancer cell lines induces a metabolic stress. A series of western blots were performed and pACC levels were monitored in order to evaluate the metabolic stress the cells experience upon glucose or Mg^{2+} depletion (Figure 4 B and C). Figure 4 A shows, under standard conditions, a slight increase in pACC levels in the shPTP4A2 MDA-MB-231 cells compared to shSCR. Upon further metabolic stress, such as low glucose conditions, 5mM glucose, the pACC effect becomes stronger when compared to high glucose conditions, 25mM glucose, where pACC levels are similar to those seen in standard conditions (Figure 4 C). Finally, the same high elevated levels in pACC are seen in PRL-2 deficient cells when the cells are subjected to low Mg^{2+} concentrations (0mM – 0.5mM) (Figure 4 B). However, under 1mM Mg^{2+}, which is the physiological concentration of free Mg^{2+} in the cell, pACC seems to behave as it does under standard culture conditions (Figure 4 B) [37-40]. Thus, PRL-2 deficient breast cancer cell lines are energetically stressed, which is assessed through the phosphorylation of ACC by active AMPK [88].

5. PRL-2 KD leads to cholesterol accumulation in the cell.

As shown in Figures 3 and 4 above, ACC and ACLY are highly phosphorylated upon PRL-2 loss. As ACLY phosphorylation leads to acetyl-CoA production, and ACC utilizes acetyl-CoA as the rate determining step in fatty acid synthesis, the inhibition of ACC through its phosphorylation should lead to acetyl-CoA accumulation in the cell [69, 70, 76, 77]. Thus, an acetyl-CoA assay kit was used to measure the total levels of acetyl-CoA in MDA-MB-231 cells induced for 48hours with doxycycline for optimal expression of shSCR and shPTP4A2s. Upon measurement of total acetyl-CoA in the cell (Figure 5 A), no significant difference in acetyl-CoA levels between the control group and the PRL-2 KD was reported. Thus, it was then hypothesized that acetyl-CoA is funneled through another pathway, the cholesterol pathway, in order to prevent acetyl-CoA toxicity. Indeed, a cholesterol assay was performed, measuring total cholesterol in MDA-MB-231 cells induced for 48hours with doxycycline. Interestingly, a significant difference between the control group and the PRL-2 KD cells was reported (Figure 5 B). Indeed, there is a significant accumulation of cholesterol in the PRL-2 KD cells, where more cholesterol accumulates in shPTP4A2$_{(3)}$ cells, 75% PRL-2 KD, than in shPTP4A2$_{(2)}$ cells, 60% PRL-2 KD, than in shSCR. Thus, a dose response phenomenon occurs, which is highly dependent on PRL-2 protein levels, which in turn strongly impacts the cholesterol synthesis pathway.

6. Loss of PRL-2 affects glucose and glutamine uptake.

As previously shown, loss of PRL-2 induces an energetic stress in the cell. To confirm that total energy levels were affected by the loss of PRL-2, a cell viability assay kit was used to measure total ATP levels within the cell after 48hours doxycycline induction. Interestingly, total ATP

levels are reduced by approximately 25% in both PRL-2 KD cell lines compared to the control group (Figure 6 A). This experiment was performed multiple times and 25% ATP reduction was reported every time in the cells lacking PRL-2. Thus, the next step in this study was to determine the metabolic pathway affected by the loss of PRL-2 in the cell, which was done using a bioprofile analyzer. Firstly, a significant decrease in glucose uptake was reported in the PRL-2 KD cell lines, which was confirmed by the decrease in lactate production, following a similar trend (Figure 6 B and C). As a reminder, lactate is produced in the cell through aerobic glycolysis, an energy generating pathway most favoured in cancer cells [61]. Furthermore, a similar effect is reported in glutamine uptake and glutamate production, where a significant reduction of glutamine uptake and glutamate production is seen in the PRL-2 KD breast cancer cells compared to their control (Figure 6 D and E). The glutamine pathway is another important metabolic pathway which favors rapid cell proliferation in cancer cells [94]. Finally, it is also interesting to notice how this reduction in nutrient uptake seems to have a dose response to PRL-2 protein levels, where a more pronounced reduction is seen in the shPTP4A2$_{(3)}$, previously shown to have a 75% decrease in PRL-2 expression compared to a less pronounced reduction in shPTP4A2$_{(2)}$, which exhibit 60% KD efficiency.

7. Loss of PRL-2 affects glucose metabolism in breast cancer.

As shown in Figure 6, loss of PRL-2 affects glucose and glutamine transport. It was then necessary to assess the effect of PRL-2 loss on glucose metabolism. Thus, Seahorse assays were performed on the inducible MDA-MB-231 breast cancer cells. After 48 hours doxycycline induction to insure optimal PRL-2 KD, cells were subjected to ECAR (Figure 7) and OCR (Figure 8) assays. The ECAR

assay shows a significant decrease in glycolytic rate and glycolytic capacity in shPTP4A2$_{(3)}$ (Figure 7 B and D). However, only a decreasing trend in glycolytic rate of shPTP4A2$_{(2)}$ is seen but no significance is reported (Figure 7 B). Glycolytic reserve seems unaffected by the loss of PRL-2 expression (Figure 7 C). The OCR assay showed a significant decrease in basal respiration, but only in shPTP4A2$_{(2)}$ (Figure 8 B). Spare respiratory capacity (SRC) and maximal respiratory capacity were also significantly decreased in the PRL-2 KD compared to control (Figure 8 C and F). ATP-linked production shows a decreasing trend, but no significance is reported (Figure 8 D). Uncoupled respiratory seems higher in the KD cells compared to control, however further experiments are required to fully understand the effect of PRL-2 loss on uncoupled respiration (Figure 8 E). Thus, taken together, Figures 7 and 8 show an effect of PRL-2 on glucose metabolism.

8. Loss of PRL-2 expression does not affect cell proliferation.

As the loss of PRL-2 has an effect on multiple main energetic pathways in breast cancer cells, it was necessary to study the proliferation rates of PRL-2 KD cells compared to their controls. As shown by Figure 4 B, MDA-MB-231 shPTP4A2 inducible breast cancer cell line are energetically stressed under low Mg^{2+} conditions when compared to the physiological levels of 1.0mM Mg^{2+}. Thus, these cells were subjected to the same Mg^{2+} conditions and a proliferation assay was performed using IncuCyte ZOOM technology. Cells were induced with doxycycline at 0hours, thus optimal shPTP4A2 expression occurred as of 48hours. It can be seen in Figure 9 that, as previously shown in the literature, cell proliferation is impeded in conditions of 0mM Mg^{2+} [47, 48]. However, PRL-2 loss does not affect the proliferation of breast cancer cells under any magnesium concentrations.

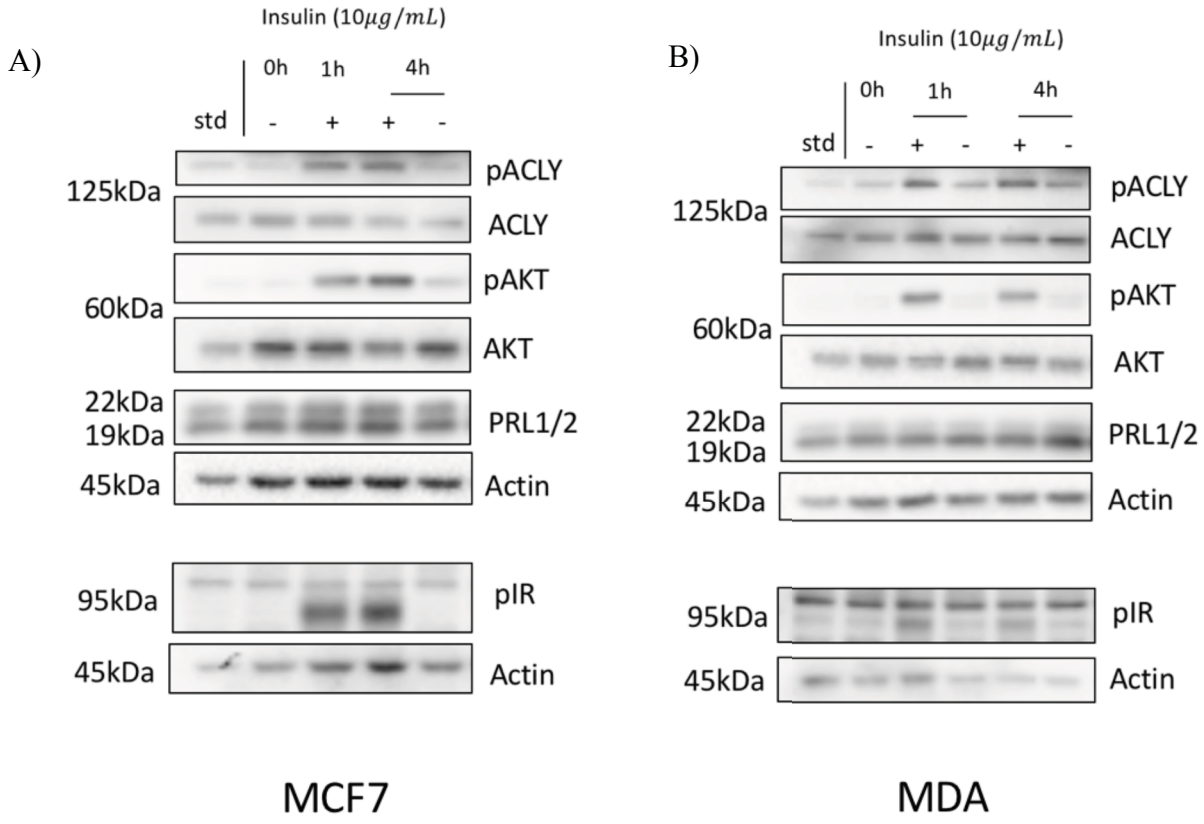

Figure 1: MCF7 and MDA-MB-231 cell lines express PRL-1 and PRL-2 and are responsive to insulin stimulation.

MCF7 and MDA-MB-231 human cell lines were starved for 24 hours to allow cell synchronization and where then treated with 10 µg/mL of insulin. Cells under standard media conditions were compared to starved and insulin stimulated conditions. Insulin stimulation was performed for 1 hour and 4 hours post starvation. A) Parental MCF7 cell line shows high expression of both PRL-1 and PRL-2 and response very well to insulin stimulation. B) Parental MDA-MB-231 cell line shows high expression of PRL-2 and some expression of PRL-1. This cell line is also responsive to insulin.

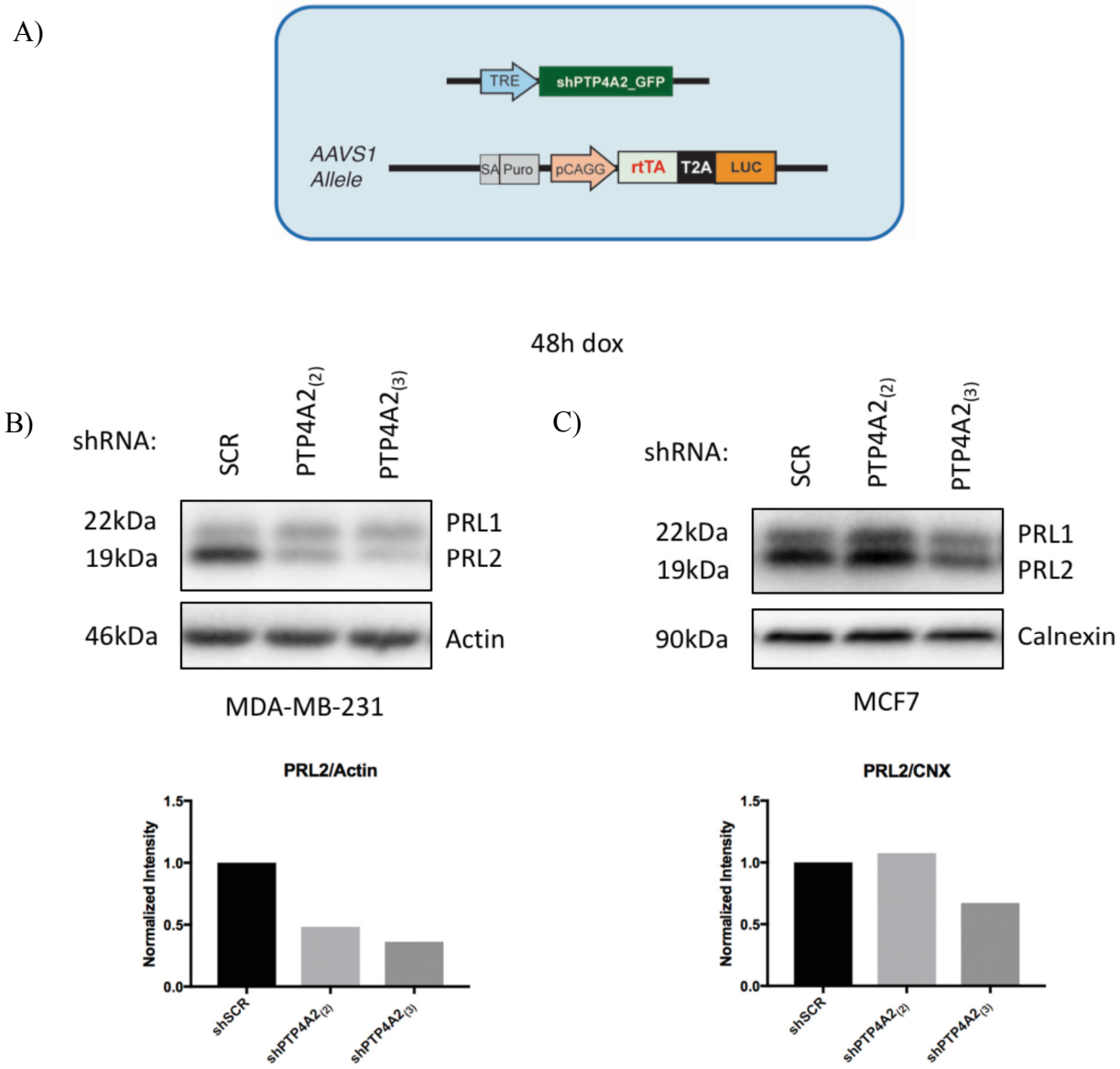

Figure 2: PRL-2 KD in breast cancer.

a) rtTA cell lines were infected with lentiviral particles containing shRNA against PTP4A2 under the control of the TRE promoter. b) MDA-MB-231 cell lines induced for 48hours with doxycycline, PRL-2 KD was confirmed by western blot. Densitometry was performed to show the efficiency of shPTP4A2 KD. c) MCF7 cell lines induced for 48hours with doxycycline, PRL-2 KD was confirmed by western blot. Densitometry was performed to show the efficiency of shPTP4A2 KD.

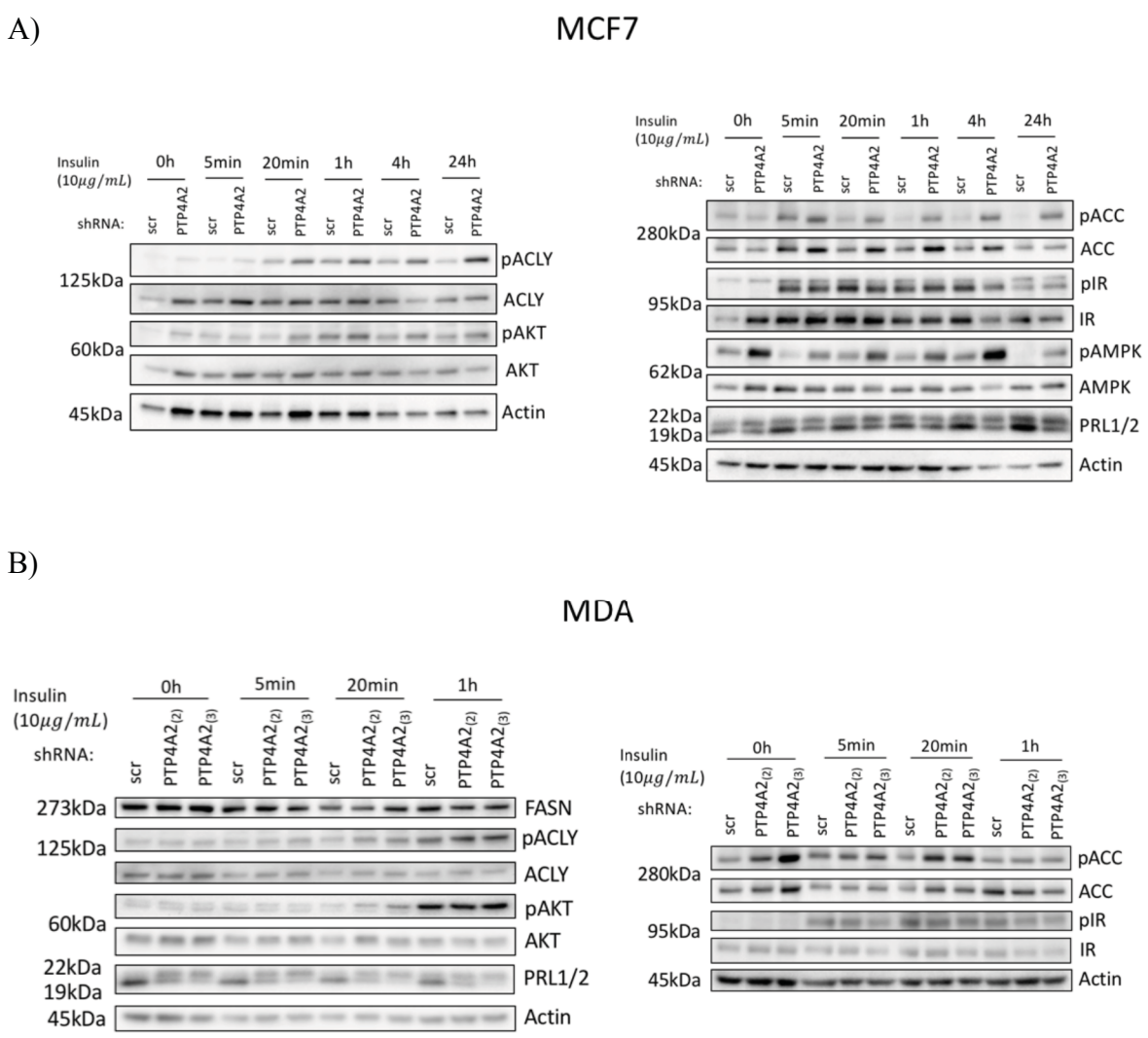

Figure 3: PRL-2 KD leads to an upregulation of phosphorylation on AKT, ACLY, AMPK and ACC.

Human breast cancer cell lines were induced for 48 hours with doxycycline leading to the expression of shPTP4A2, after which the cells were starved for 24 hours in the presence of doxycycline allowing to maintain PRL-2 KD. Then, the cells were stimulated with 10µg/mL of insulin over time and lipid synthesis protein levels were assessed through western blot. a) MCF7 human cell line b) MDA-MB-231 human cell line. Shown is a representative experiment. These results have been confirmed through western blot multiple times.

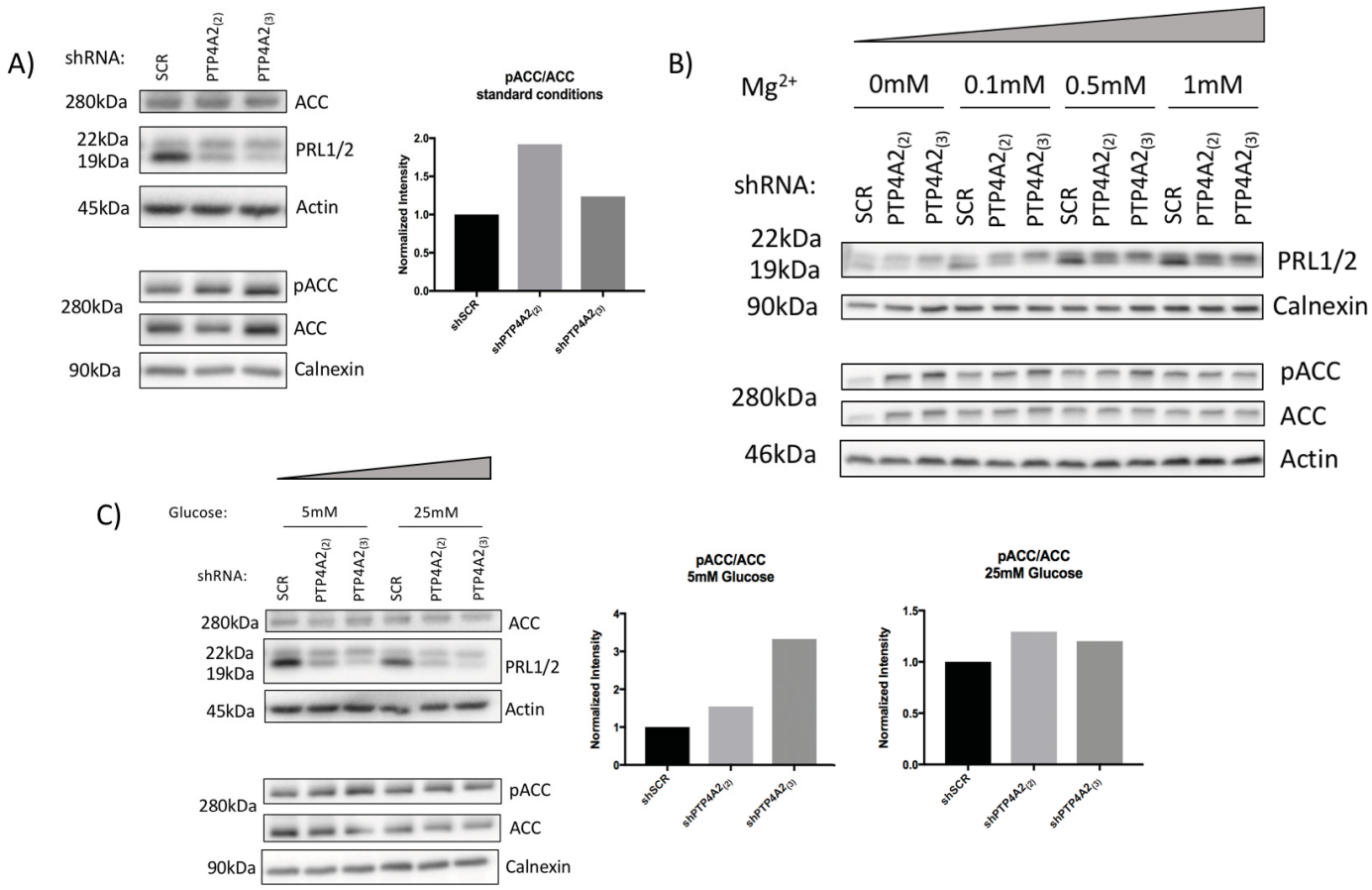

Figure 4: PRL-2 KD induces an acute energetic stress in breast cancer.

MDA-MB-231 cell lines were induced for 48 hours with dox leading to optimal expression of shPTP4A2 and shSCR. A) pACC expression was assessed under standard conditions, B) pACC expression was assessed under different magnesium concentrations for 6 hours post doxycycline induction and C) pACC expression was assessed under low (5mM) or high (25mM) glucose conditions for 6 hours post 48h dox induction. Densitometry measurements were performed to further confirm pACC/ACC expression. These are representative western blots. These experiments have been performed multiple times.

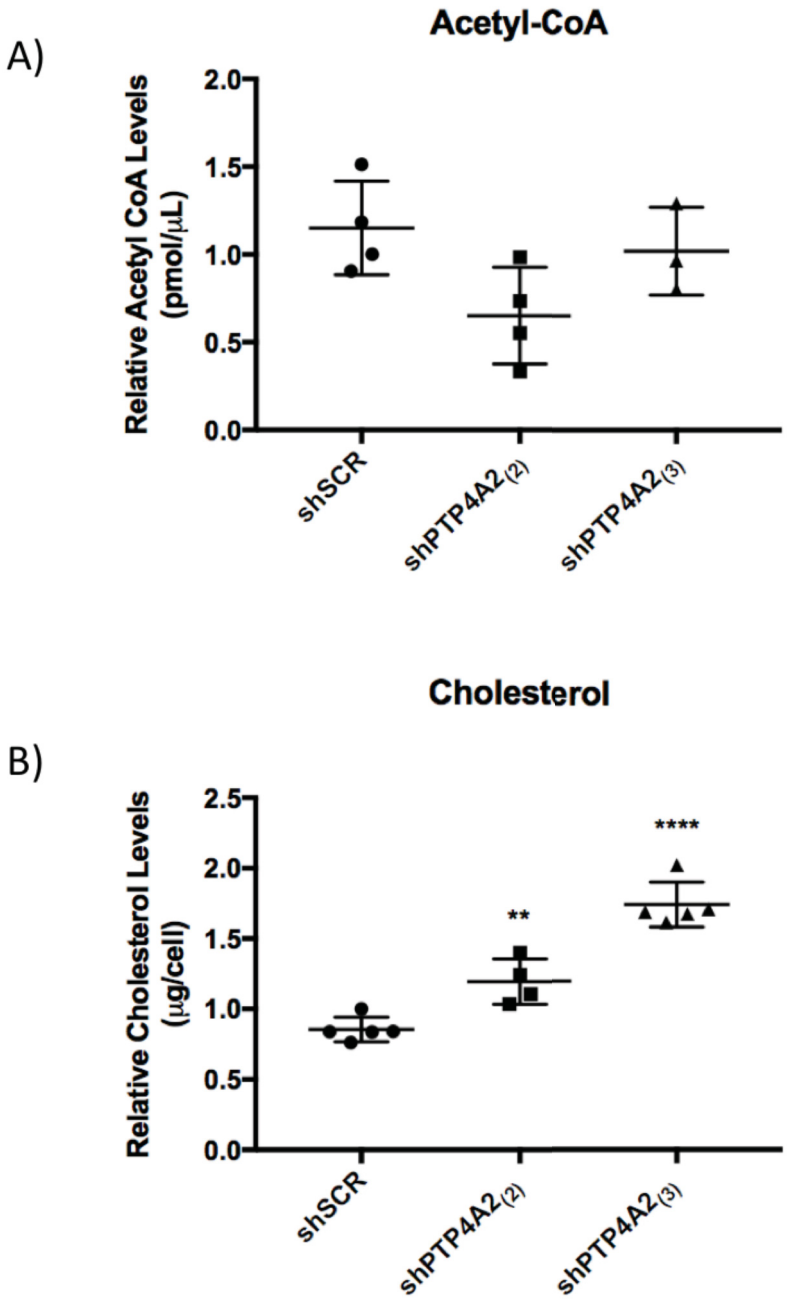

Figure 5: Loss of PRL-2 leads to increased cholesterol levels inside the cell.

MDA-MB-231 cell lines were induced for 48 hours with dox leading to the expression of shPTP4A2. A) Acetyl-CoA levels were measure, each sample contained $2x10^6$ cells. Shown is the relative Acetyl-CoA amount compared to shSCR. B) Cholesterol levels measured in the cell and normalized to total cell number. This experiment was performed three times. One-way ANOVA statistical analysis was performed. **$p < 0.01$, **** $p < 0.0001$.

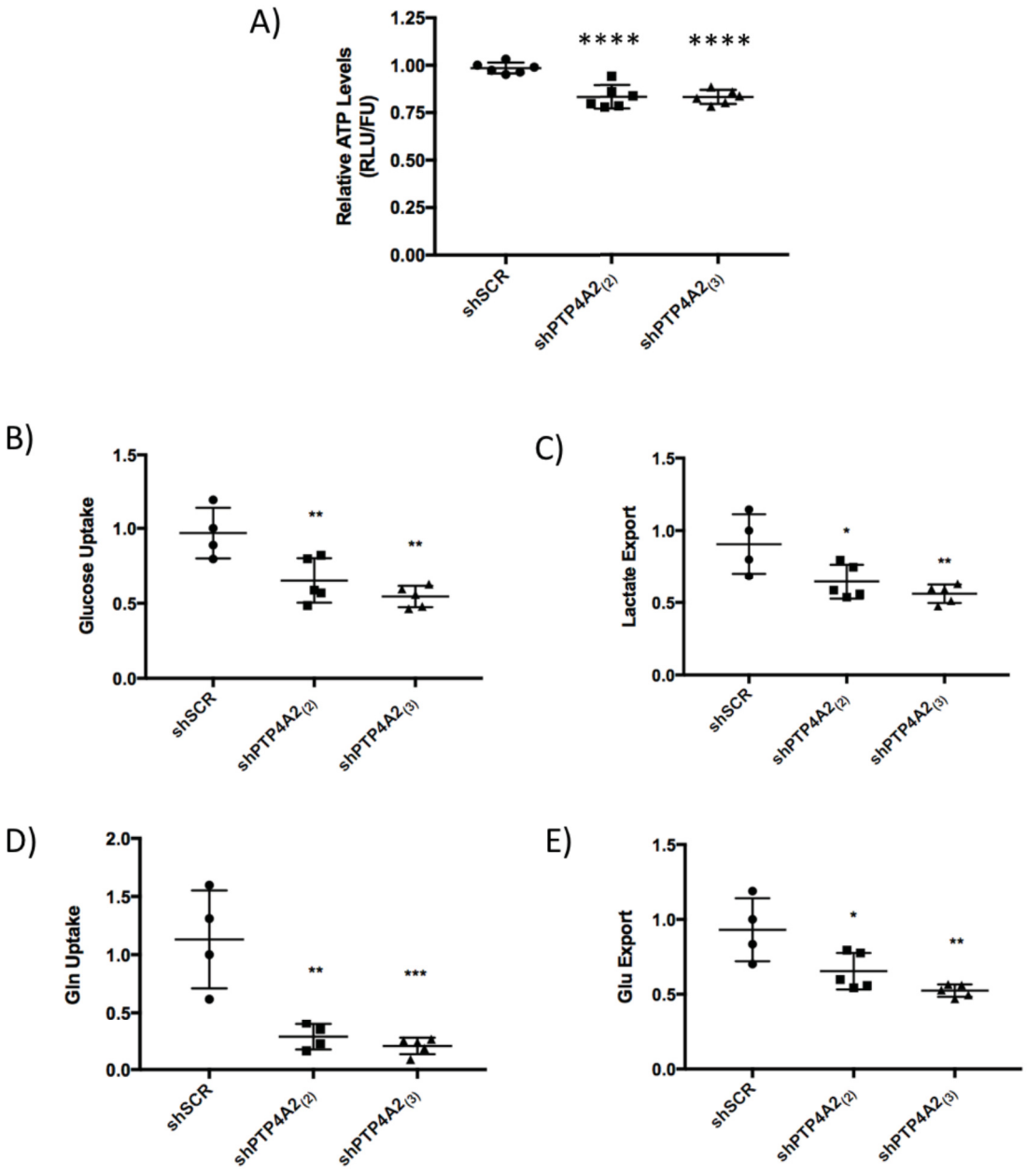

Figure 6: PRL-2 KD alters cell energetics by affecting glucose and glutamine metabolism. MDA-MB-231 cell lines were induced for 48 hours with dox leading to the expression of shPTP4A2. A) Total ATP levels were measured and were normalized to total DNA content. Shown is the relative total ATP amount compared to shSCR. B) Glucose uptake C) Lactate export D) Glutamine uptake and E) Glutamate export were measured and normalized to total cell

number. Shown are relative amounts compared to shSCR. One-way ANOVA statistical analysis was performed. *p < 0.05, **p < 0.01, ***p < 0.0005, ****p < 0.0001.

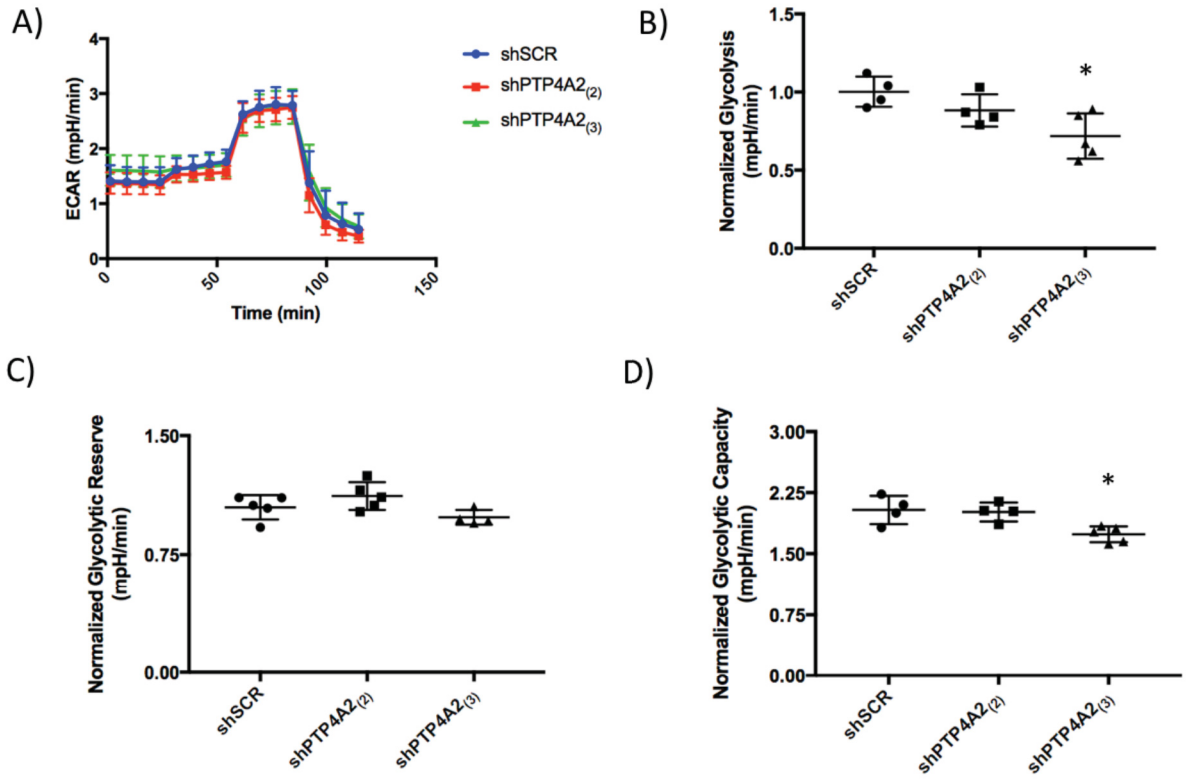

Figure 7: Loss of PRL-2 affects glycolysis in breast cancer.

MDA-MB-231 cell lines were induced for 48 hours with dox leading to the expression of shPTP4A2 before running the ECAR assay. A) ECAR profile B) Glycolytic rate normalized to total DNA content C) Glycolytic reserve normalized to total DNA content D) Glycolytic capacity normalized to total DNA content. This is a representative experiment, three separate experiments were performed, all showing a similar trend. One-way ANOVA statistical analysis was performed. *$p < 0.05$.

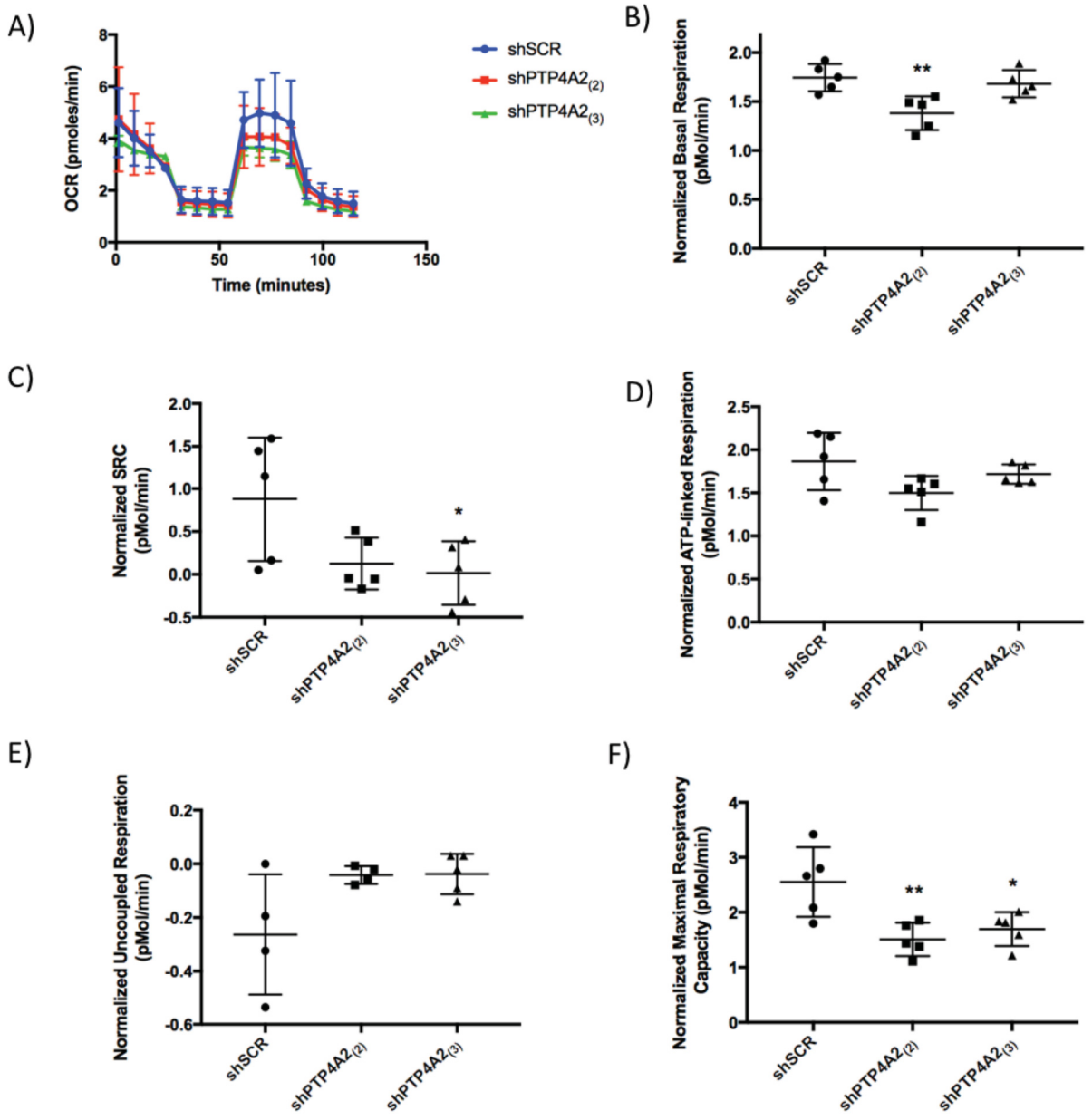

Figure 8: Loss of PRL-2 affects oxidative phosphorylation in breast cancer.

MDA-MB-231 cell lines were induced for 48 hours with dox leading to the expression of shPTP4A2 before running the OCR assay. A) OCR profile B) Basal respiration rate, C) Spare respiratory capacity, D) ATP-linked respiration, E) Uncoupled respiration and F) Maximal Respiratory Capacity, all normalized to total DNA content. This is a representative experiment, two separate experiments were performed, both showing a similar trend. One-way ANOVA statistical analysis was performed. *$p < 0.05$, **$p < 0.01$.

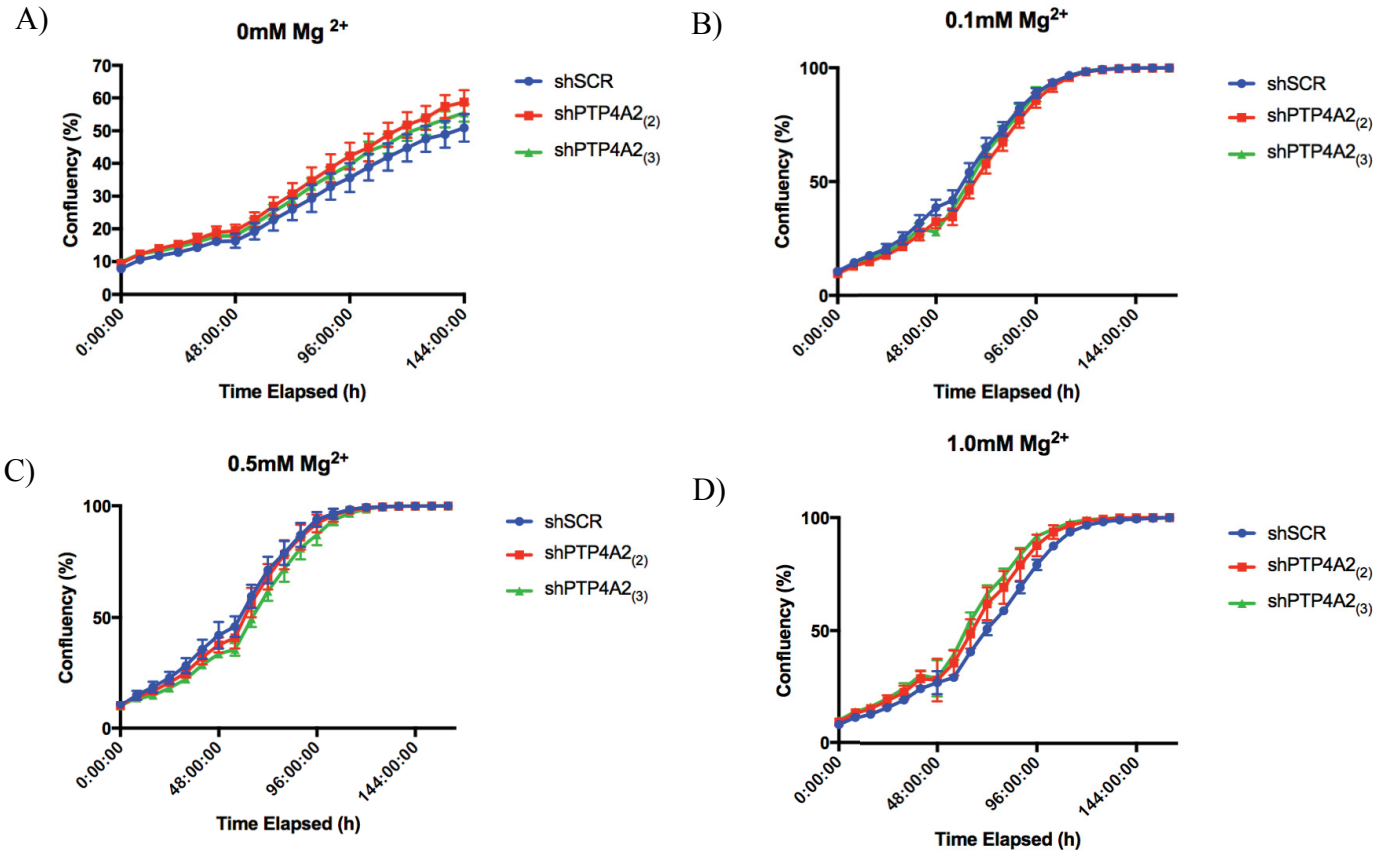

Figure 9: The effect of PRL-2 on cell proliferation in breast cancer.

MDA-MB-231 cell lines were induced with dox at time 0h allowing for the expression of shSCR or shPTP4A2. The cells were under dox treatment for the full length of the experiment. A) Proliferation profile under 0mM Mg^{2+} conditions B) Proliferation profile under 0.1mM Mg^{2+} conditions C) Proliferation profile under 0.5mM Mg^{2+} conditions D) Proliferation profile under 1.0mM Mg^{2+} conditions. One-way ANOVA statistical analysis was performed. *$p < 0.05$, **$p < 0.01$.

DISCUSSION

Our group has previously shown that PRL-2 is overexpressed in primary breast tumours and in metastatic lymph nodes, and that its overexpression in a breast cancer transgenic mouse increased tumour progression [21, 29]. Furthermore, more recent studies have linked PRL-2 with fatty acid synthesis and TCA cycle intermediates accumulation [36]. Thus, this study's main objective was to determine the role of PRL-2 in breast cancer metabolism.

It was first demonstrated that both MCF7 and MDA-MB-231 human breast cancer cell lines expressed PRL-1 and PRL-2. As expected, upon PRL-2 KD, PRL-1 protein levels increased in order to compensate for the loss of PRL-2 [34, 35]. Interestingly, this compensation is not apparent in the MCF7 cell line as PRL-1 basal levels are already very high, whereas PRL-1 compensation is much more apparent in the MDA-MB-231 cell line, which has very little PRL-1 compared to PRL-2 levels. This compensation by PRL-1 is essential as PRL-1/PRL-2 double KO has been shown to be embryonic lethal, meaning that expression of either PRL-1 or PRL-2 is required for survival [34].

Furthermore, an inducible shRNA model targeting PRL-2 was selected in order to study the acute metabolic effect upon loss of PRL-2. Indeed, an inducible model allows to study the effects of PRL-2 loss prior metabolic adaptation of the cells. Also, as PRL-2 is overexpressed in breast cancer, it was determined that an overexpression model would not be helpful for this study [21].

The first experiment performed in the inducible breast cancer model showed, in both MCF7 and MDA-MB-231 cell lines, an increase in ACC phosphorylation in the PRL-2 KD cells suggesting that PRL-2 plays a role in cell energetics, as ACC is directly phosphorylated by AMPK, an energy

sensor [88]. A major increase of pACLY in the PRL-2 KD cells was also reported in the MCF7 cell lines. Although a similar effect is seen in the MDA-MB-231 cell line after 20 minutes insulin stimulation, the effect is not as pronounced as in the MCF7 cell lines. It was hypothesized that the more pronounced effect seen in MCF7 is due to the lack of compensation by PRL-1. Thus, MCF7 depend on PRL-1 and PRL-2 expression much more than the MDA-MB-231 cells do. However, since the MDA-MB-231 model shows a stronger KD efficiency, it was decided that the MDA-MB-231 inducible cells only will be used for further studies.

As AMPK activity in the MDA-MB-231 cells seems strongest following serum starvation, it was hypothesized that further metabolic stress, such as nutrient deprivation, glucose deprivation or Mg^{2+} deprivation would lead to increased metabolic stress in cells lacking PRL-2. Indeed, an increase in AMPK activity was reported through increased pACC in the PRL-2 KD cells upon further metabolically stress induced by low glucose or low Mg^{2+} levels, confirming that PRL-2 expression is linked to cell metabolism.

However, it is still unknown where exactly PRL-2 action occurs within the many metabolic pathways. PRL-2 loss leads to increased pACC, which is a marker for energetic stress but ACC is also a rate determining step in fatty acid synthesis and its phosphorylation is inhibitory [70, 76, 77]. Furthermore, ACC uses acetyl-CoA synthesized by pACLY to produce malonyl-CoA [70, 76, 77], suggesting that ACC inhibition and ACLY activation will lead to acetyl-CoA accumulation, which has been shown to lead to epithelial-mesenchymal transition and metastasis induction in breast cancer [99]. However, no significant difference in acetyl-CoA levels was reported upon PRL-2 loss. Thus, as the cholesterol pathway also channels acetyl-CoA to make cholesterol, cholesterol levels were measured [69]. Indeed, an accumulation of cholesterol was reported in

both PRL-2 KD cells, which also seems to be PRL-2 dependent, as lower level of PRL-2 expression lead to higher cholesterol levels inside the cell. Thus, it is assumed that PRL-2 loss leads to inhibition of the fatty acid synthesis pathway, which will lead indirectly to cholesterol production to avoid acetyl-CoA accumulation. However, further experiments to assess enzymatic activity within the cholesterol pathway should be performed. Acetyl-CoA and malonyl-CoA levels should also be measured using techniques such as gas chromatography-mass spectrometry (GC-MS) and liquid chromatography-mass spectrometry (LC-MS), which are much more sensitive to these molecules.

As pACC is used to report metabolic stress, it was also important to study the effect of PRL-2 loss on the other major metabolic pathways leading to ATP synthesis, such as glucose and glutamine metabolism [53, 94, 95]. Thus, an ATP assay was first performed and a 25% decrease in total ATP levels was reported in the PRL-2 KD cells, supporting the increase in AMPK activity and that loss of PRL-2 does lead to cellular metabolic stress. This was consistent with a decrease in glucose uptake and lactate production, suggesting a decrease in aerobic glycolysis, main energy producer in cancer cells, as stated by the Warburg effect [61]. Recent studies have linked AMPK activation to PGC1α/ERRα metabolic reprogramming leading to reduced aerobic glycolysis reported by low lactate production [100]. Furthermore, as PRL-2 has been identified as a target of ERRα, it can be hypothesized that PRL-2 might also play a role in PGC1α/ERRα metabolic reprogramming [28]. As glucose metabolism is the major fuel in the cell, Seahorse assays were performed to confirm the PRL-2 effect on glucose metabolism. In the ECAR assay, allowing to assess glycolysis, a decrease in glycolytic rate and total glycolytic capacity was reported, indicating that upon PRL-2 KD, less ATP is produced by glycolysis and it becomes

harder for the cell to respond to further glycolytic stress. Furthermore, OCR assay showed a decrease in basal respiration, spare respiratory capacity and maximum respiration also indicating that ATP production at the mitochondrial level is hindered by the loss of PRL-2. Interestingly, a decrease in glutamine uptake, followed by a decrease in glutamate was also observed. Recent studies have also linked PGC1α expression to glutamine metabolism, suggesting a putative connection between PRL-2 action in PGC1α metabolic reprogramming [101]. Both glucose and glutamine pathways are major energetic pathways leading to ATP production and seem to be highly impaired by the loss of PRL-2 [53, 94, 95]. Even more fascinating, the decrease reported was dependent on PRL-2 levels within the cell, as was the case in the cholesterol experiment. This further suggests that PRL expression might be crucial in breast cancer metabolism.

As substantial evidence on the effect of PRL-2 on metabolic stress was shown, it was hypothesized that this must also have an effect on cell proliferation. A cell proliferation assay was performed under varying Mg^{2+} concentration conditions to see if further metabolic stress would have a stronger effect on cell proliferation. Furthermore, as PRL-2 has been linked to Mg^{2+} in the literature, it was hypothesized that all effects seen on the varying metabolic pathways within the cell were due to the decrease in Mg^{2+} levels within the cell due to loss of PRL-2 [29]. Indeed, multiple glycolytic enzymes, such as hexokinase, are shown to rely on Mg^{2+} levels for their action [55]. Thus, modulation Mg^{2+} levels while knocking down PRL-2 should have a great effect on breast cancer cell lines. Surprisingly, no difference in proliferation was reported under low Mg^{2+} conditions, nor normal physiological Mg^{2+} levels. This suggests that

PRL-2 effect on metabolism might not be solely due to Mg^{2+}. Furthermore, there must be some other mechanism that comes and rescues the effect of the loss of PRL-2.

As there is already strong evidence suggesting the involvement of PRL-2 in lipid metabolism, it is thought that fatty acid oxidation might be highly used to compensate for the effect on decreased glucose and glutamine metabolism.

Thus, further experiments must be performed to fully understand biological effects of PRL-2 on breast cancer metabolism and to determine a mechanism of action, currently unknown. Fatty acid oxidation can be easily assessed by looking at CPT1 and PPARα expression as well as malonyl-CoA levels [70, 76, 77]. Using inhibitors against fatty acid oxidation could lead to altered cell proliferation or survival, confirming the importance of the beta oxidation pathway in PRL-2 KD cells. Carbon flux experiments will be important to assess TCA cycle activity and intermediate accumulation, as Seahorse experiments have shown impaired mitochondrial function. Similarly, as the PRL-2 KD cells uptake less glucose and glutamine, modulating the availability of both of these extracellular metabolites might as well affect cell survival. Finally, 3D culture and xenograft assay could be insightful as cells are subjected to more stringent conditions representative of a tumor environment that might allow to report differences in proliferation upon PRL-2 KD.

CONCLUSION

Taken together, this thesis shows that PRL-2 does have a role in breast cancer metabolism, which can potentially be exploited for therapeutic use after further studies determine a mechanism of action. As loss of PRL-2 leads to an energetic stress in the cell through impaired glucose and glutamine uptake, it is thought that overexpression of PRL-2 in cancer facilitates metabolic reprogramming. Indeed, PRL-2 is overexpressed in multiple cancers, including breast cancer and is strongly associated with cancer progression and metastasis [21, 29]. Thus, this study suggests that overexpression of PRL-2 will lead to cancer progression by stimulating glucose and glutamine pathways, thus producing higher ATP levels, allowing the cancer cells to produce enough energy for their main cellular processes.

REFERENCES

1. Beltrao, P., et al., *Evolution and functional cross-talk of protein post-translational modifications.* Mol Syst Biol, 2013. **9**: p. 714.
2. Cohen, P., *Protein phosphorylation and hormone action.* Proc R Soc Lond B Biol Sci, 1988. **234**(1275): p. 115-44.
3. Cohen, P.T., *Novel protein serine/threonine phosphatases: variety is the spice of life.* Trends Biochem Sci, 1997. **22**(7): p. 245-51.
4. Denu, J.M. and J.E. Dixon, *Protein tyrosine phosphatases: mechanisms of catalysis and regulation.* Curr Opin Chem Biol, 1998. **2**(5): p. 633-41.
5. Alonso, A., et al., *Protein tyrosine phosphatases in the human genome.* Cell, 2004. **117**(6): p. 699-711.
6. Streuli, M., et al., *Distinct functional roles of the two intracellular phosphatase like domains of the receptor-linked protein tyrosine phosphatases LCA and LAR.* EMBO J, 1990. **9**(8): p. 2399-407.
7. Pulido, R., A. Zuniga, and A. Ullrich, *PTP-SL and STEP protein tyrosine phosphatases regulate the activation of the extracellular signal-regulated kinases ERK1 and ERK2 by association through a kinase interaction motif.* EMBO J, 1998. **17**(24): p. 7337-50.
8. Guan, K.L., S.S. Broyles, and J.E. Dixon, *A Tyr/Ser protein phosphatase encoded by vaccinia virus.* Nature, 1991. **350**(6316): p. 359-62.
9. Ostman, A., C. Hellberg, and F.D. Bohmer, *Protein-tyrosine phosphatases and cancer.* Nat Rev Cancer, 2006. **6**(4): p. 307-20.
10. Julien, S.G., et al., *Inside the human cancer tyrosine phosphatome.* Nat Rev Cancer, 2011. **11**(1): p. 35-49.

11. Tonks, N.K., *Redox redux: revisiting PTPs and the control of cell signaling.* Cell, 2005. **121**(5): p. 667-70.

12. Cates, C.A., et al., *Prenylation of oncogenic human PTP(CAAX) protein tyrosine phosphatases.* Cancer Lett, 1996. **110**(1-2): p. 49-55.

13. Gjorloff-Wingren, A., et al., *Subcellular localization of intracellular protein tyrosine phosphatases in T cells.* Eur J Immunol, 2000. **30**(8): p. 2412-21.

14. Sun, J.P., et al., *Phosphatase activity, trimerization, and the C-terminal polybasic region are all required for PRL1-mediated cell growth and migration.* J Biol Chem, 2007. **282**(39): p. 29043-51.

15. Bessette, D.C., D. Qiu, and C.J. Pallen, *PRL PTPs: mediators and markers of cancer progression.* Cancer Metastasis Rev, 2008. **27**(2): p. 231-52.

16. Fagerberg, L., et al., *Analysis of the human tissue-specific expression by genome-wide integration of transcriptomics and antibody-based proteomics.* Mol Cell Proteomics, 2014. **13**(2): p. 397-406.

17. Duff, M.O., et al., *Genome-wide identification of zero nucleotide recursive splicing in Drosophila.* Nature, 2015. **521**(7552): p. 376-9.

18. Hardy, S., et al., *Physiological and oncogenic roles of the PRL phosphatases.* FEBS J, 2018.

19. Rubin, H., *Central role for magnesium in coordinate control of metabolism and growth in animal cells.* Proc Natl Acad Sci U S A, 1975. **72**(9): p. 3551-5.

20. Achiwa, H. and J.S. Lazo, *PRL-1 tyrosine phosphatase regulates c-Src levels, adherence, and invasion in human lung cancer cells.* Cancer Res, 2007. **67**(2): p. 643-50.

21. Hardy, S., et al., *Overexpression of the protein tyrosine phosphatase PRL-2 correlates with breast tumor formation and progression.* Cancer Res, 2010. **70**(21): p. 8959-67.

22. Kato, H., et al., *High expression of PRL-3 promotes cancer cell motility and liver metastasis in human colorectal cancer: a predictive molecular marker of metachronous liver and lung metastases.* Clin Cancer Res, 2004. **10**(21): p. 7318-28.

23. Li, Z., et al., *Inhibition of PRL-3 gene expression in gastric cancer cell line SGC7901 via microRNA suppressed reduces peritoneal metastasis.* Biochem Biophys Res Commun, 2006. **348**(1): p. 229-37.

24. Polato, F., et al., *PRL-3 phosphatase is implicated in ovarian cancer growth.* Clin Cancer Res, 2005. **11**(19 Pt 1): p. 6835-9.

25. Qian, F., et al., *PRL-3 siRNA inhibits the metastasis of B16-BL6 mouse melanoma cells in vitro and in vivo.* Mol Med, 2007. **13**(3-4): p. 151-9.

26. Dong, J., et al., *MicroRNA-26a inhibits cell proliferation and invasion of cervical cancer cells by targeting protein tyrosine phosphatase type IVA 1.* Mol Med Rep, 2014. **10**(3): p. 1426-32.

27. Dumaual, C.M., et al., *Tissue-specific alterations of PRL-1 and PRL-2 expression in cancer.* Am J Transl Res, 2012. **4**(1): p. 83-101.

28. Deblois, G., et al., *Genome-wide identification of direct target genes implicates estrogen-related receptor alpha as a determinant of breast cancer heterogeneity.* Cancer Res, 2009. **69**(15): p. 6149-57.

29. Hardy, S., et al., *The protein tyrosine phosphatase PRL-2 interacts with the magnesium transporter CNNM3 to promote oncogenesis.* Oncogene, 2015. **34**(8): p. 986-95.

30. Gimenez-Mascarell, P., et al., *Structural Basis of the Oncogenic Interaction of Phosphatase PRL-1 with the Magnesium Transporter CNNM2.* J Biol Chem, 2017. **292**(3): p. 786-801.

31. Corral-Rodriguez, M.A., et al., *Nucleotide binding triggers a conformational change of the CBS module of the magnesium transporter CNNM2 from a twisted towards a flat structure.* Biochem J, 2014. **464**(1): p. 23-34.

32. Hirata, Y., et al., *Mg2+-dependent interactions of ATP with the cystathionine-beta-synthase (CBS) domains of a magnesium transporter.* J Biol Chem, 2014. **289**(21): p. 14731-9.

33. de Baaij, J.H., et al., *Membrane topology and intracellular processing of cyclin M2 (CNNM2).* J Biol Chem, 2012. **287**(17): p. 13644-55.

34. Bai, Y., et al., *Role of phosphatase of regenerating liver 1 (PRL1) in spermatogenesis.* Sci Rep, 2016. **6**: p. 34211.

35. Dong, Y., et al., *Phosphatase of regenerating liver 2 (PRL2) deficiency impairs Kit signaling and spermatogenesis.* J Biol Chem, 2014. **289**(6): p. 3799-810.

36. Uetani, N., et al., *PRL2 links magnesium flux and sex-dependent circadian metabolic rhythms.* JCI Insight, 2017. **2**(13).

37. Romani, A. and A. Scarpa, *Regulation of cell magnesium.* Arch Biochem Biophys, 1992. **298**(1): p. 1-12.

38. Wolf, F.I., et al., *Cell physiology of magnesium.* Mol Aspects Med, 2003. **24**(1-3): p. 11-26.

39. Wolf, F.I. and A. Cittadini, *Chemistry and biochemistry of magnesium.* Mol Aspects Med, 2003. **24**(1-3): p. 3-9.

40. Jung, D.W., L. Apel, and G.P. Brierley, *Matrix free Mg2+ changes with metabolic state in isolated heart mitochondria.* Biochemistry, 1990. **29**(17): p. 4121-8.

41. Romani, A., *Regulation of magnesium homeostasis and transport in mammalian cells.* Arch Biochem Biophys, 2007. **458**(1): p. 90-102.

42. Grubbs, R.D. and M.E. Maguire, *Magnesium as a regulatory cation: criteria and evaluation.* Magnesium, 1987. **6**(3): p. 113-27.

43. Romani, A.M. and M.E. Maguire, *Hormonal regulation of Mg2+ transport and homeostasis in eukaryotic cells.* Biometals, 2002. **15**(3): p. 271-83.

44. Romani, A.M. and A. Scarpa, *Regulation of cellular magnesium.* Front Biosci, 2000. **5**: p. D720-34.

45. Fatholahi, M., et al., *Relationship between total and free cellular Mg(2+) during metabolic stimulation of rat cardiac myocytes and perfused hearts.* Arch Biochem Biophys, 2000. **374**(2): p. 395-401.

46. Kubota, T., et al., *Mitochondria are intracellular magnesium stores: investigation by simultaneous fluorescent imagings in PC12 cells.* Biochim Biophys Acta, 2005. **1744**(1): p. 19-28.

47. Garfinkel, D. and L. Garfinkel, *Magnesium and regulation of carbohydrate metabolism at the molecular level.* Magnesium, 1988. **7**(5-6): p. 249-61.

48. Otto, M., et al., *A mathematical model for the influence of fructose 6-phosphate, ATP, potassium, ammonium and magnesium on the phosphofructokinase from rat erythrocytes.* Eur J Biochem, 1974. **49**(1): p. 169-78.

49. Fagan, T.E. and A. Romani, *Activation of Na(+)- and Ca(2+)-dependent Mg(2+) extrusion by alpha(1)- and beta-adrenergic agonists in rat liver cells.* Am J Physiol Gastrointest Liver Physiol, 2000. **279**(5): p. G943-50.

50. Reed, G., et al., *Lack of insulin impairs Mg2+ homeostasis and transport in cardiac cells of streptozotocin-injected diabetic rats.* J Cell Biochem, 2008. **104**(3): p. 1034-53.

51. Scarpa, A. and F.J. Brinley, *In situ measurements of free cytosolic magnesium ions.* Fed Proc, 1981. **40**(12): p. 2646-52.

52. Luthi, D., D. Gunzel, and J.A. McGuigan, *Mg-ATP binding: its modification by spermine, the relevance to cytosolic Mg2+ buffering, changes in the intracellular ionized Mg2+ concentration and the estimation of Mg2+ by 31P-NMR.* Exp Physiol, 1999. **84**(2): p. 231-52.

53. Wallace, D.C., W. Fan, and V. Procaccio, *Mitochondrial energetics and therapeutics.* Annu Rev Pathol, 2010. **5**: p. 297-348.

54. Bacci, G., et al., *Prognostic significance of serum lactic acid dehydrogenase in Ewing's tumor of bone.* Ric Clin Lab, 1985. **15**(1): p. 89-96.

55. Akram, M., *Mini-review on glycolysis and cancer.* J Cancer Educ, 2013. **28**(3): p. 454-7.

56. Fernie, A.R., et al., *Fructose 2,6-bisphosphate activates pyrophosphate: fructose-6-phosphate 1-phosphotransferase and increases triose phosphate to hexose phosphate cycling in heterotrophic cells.* Planta, 2001. **212**(2): p. 250-63.

57. Mulquiney, P.J., W.A. Bubb, and P.W. Kuchel, *Model of 2,3-bisphosphoglycerate metabolism in the human erythrocyte based on detailed enzyme kinetic equations: in vivo kinetic characterization of 2,3-bisphosphoglycerate synthase/phosphatase using 13C and 31P NMR.* Biochem J, 1999. **342 Pt 3**: p. 567-80.

58. Allard, M.F., et al., *Contribution of oxidative metabolism and glycolysis to ATP production in hypertrophied hearts.* Am J Physiol, 1994. **267**(2 Pt 2): p. H742-50.

59. Owen, O.E., S.C. Kalhan, and R.W. Hanson, *The key role of anaplerosis and cataplerosis for citric acid cycle function.* J Biol Chem, 2002. **277**(34): p. 30409-12.

60. Zheng, J., *Energy metabolism of cancer: Glycolysis versus oxidative phosphorylation (Review).* Oncol Lett, 2012. **4**(6): p. 1151-1157.

61. Vander Heiden, M.G., L.C. Cantley, and C.B. Thompson, *Understanding the Warburg effect: the metabolic requirements of cell proliferation.* Science, 2009. **324**(5930): p. 1029-33.

62. Kroemer, G. and J. Pouyssegur, *Tumor cell metabolism: cancer's Achilles' heel.* Cancer Cell, 2008. **13**(6): p. 472-82.

63. Baysal, B.E., et al., *Mutations in SDHD, a mitochondrial complex II gene, in hereditary paraganglioma.* Science, 2000. **287**(5454): p. 848-51.

64. Tomlinson, I.P., et al., *Germline mutations in FH predispose to dominantly inherited uterine fibroids, skin leiomyomata and papillary renal cell cancer.* Nat Genet, 2002. **30**(4): p. 406-10.

65. Yan, H., et al., *IDH1 and IDH2 mutations in gliomas.* N Engl J Med, 2009. **360**(8): p. 765-73.

66. Divakaruni, A.S., et al., *Analysis and interpretation of microplate-based oxygen consumption and pH data.* Methods Enzymol, 2014. **547**: p. 309-54.

67. Zimmet, P., K.G. Alberti, and J. Shaw, *Global and societal implications of the diabetes epidemic.* Nature, 2001. **414**(6865): p. 782-7.

68. Bauer, D.E., et al., *ATP citrate lyase is an important component of cell growth and transformation.* Oncogene, 2005. **24**(41): p. 6314-22.

69. Chypre, M., N. Zaidi, and K. Smans, *ATP-citrate lyase: a mini-review.* Biochem Biophys Res Commun, 2012. **422**(1): p. 1-4.

70. McGarry, J.D., *Banting lecture 2001: dysregulation of fatty acid metabolism in the etiology of type 2 diabetes.* Diabetes, 2002. **51**(1): p. 7-18.

71. Latasa, M.J., et al., *Occupancy and function of the -150 sterol regulatory element and -65 E-box in nutritional regulation of the fatty acid synthase gene in living animals.* Mol Cell Biol, 2003. **23**(16): p. 5896-907.

72. Pearce, N.J., et al., *The role of ATP citrate-lyase in the metabolic regulation of plasma lipids. Hypolipidaemic effects of SB-204990, a lactone prodrug of the potent ATP citrate-lyase inhibitor SB-201076.* Biochem J, 1998. **334 (Pt 1)**: p. 113-9.

73. Wellen, K.E., et al., *ATP-citrate lyase links cellular metabolism to histone acetylation.* Science, 2009. **324**(5930): p. 1076-80.

74. Fukuda, H., A. Katsurada, and N. Iritani, *Effects of nutrients and hormones on gene expression of ATP citrate-lyase in rat liver.* Eur J Biochem, 1992. **209**(1): p. 217-22.

75. Migita, T., et al., *ATP citrate lyase: activation and therapeutic implications in non-small cell lung cancer.* Cancer Res, 2008. **68**(20): p. 8547-54.

76. Abu-Elheiga, L., et al., *Continuous fatty acid oxidation and reduced fat storage in mice lacking acetyl-CoA carboxylase 2.* Science, 2001. **291**(5513): p. 2613-6.

77. Abu-Elheiga, L., et al., *Acetyl-CoA carboxylase 2 mutant mice are protected against obesity and diabetes induced by high-fat/high-carbohydrate diets.* Proc Natl Acad Sci U S A, 2003. **100**(18): p. 10207-12.

78. Kim, K.H., *Regulation of mammalian acetyl-coenzyme A carboxylase.* Annu Rev Nutr, 1997. **17**: p. 77-99.

79. Mao, J., S.S. Chirala, and S.J. Wakil, *Human acetyl-CoA carboxylase 1 gene: presence of three promoters and heterogeneity at the 5'-untranslated mRNA region.* Proc Natl Acad Sci U S A, 2003. **100**(13): p. 7515-20.

80. Zhang, Y., L. Yin, and F.B. Hillgartner, *SREBP-1 integrates the actions of thyroid hormone, insulin, cAMP, and medium-chain fatty acids on ACCalpha transcription in hepatocytes.* J Lipid Res, 2003. **44**(2): p. 356-68.

81. Iritani, N., *Nutritional and hormonal regulation of lipogenic-enzyme gene expression in rat liver.* Eur J Biochem, 1992. **205**(2): p. 433-42.

82. Shimano, H., et al., *Sterol regulatory element-binding protein-1 as a key transcription factor for nutritional induction of lipogenic enzyme genes.* J Biol Chem, 1999. **274**(50): p. 35832-9.

83. Lane, M.D., J. Moss, and S.E. Polakis, *Acetyl coenzyme A carboxylase.* Curr Top Cell Regul, 1974. **8**(0): p. 139-95.

84. Vagelos, P.R., A.W. Alberts, and D.B. Martin, *Studies on the mechnism of activation of acetyl coenzyme A carboxylase by citrate.* J Biol Chem, 1963. **238**: p. 533-40.

85. Boone, A.N., et al., *Bimodal activation of acetyl-CoA carboxylase by glutamate.* J Biol Chem, 2000. **275**(15): p. 10819-25.

86. Ogiwara, H., et al., *Inhibition of rat-liver acetyl-coenzyme-A carboxylase by palmitoyl-coenzyme A. Formation of equimolar enzyme-inhibitor complex.* Eur J Biochem, 1978. **89**(1): p. 33-41.

87. Hardie, D.G., *Regulation of fatty acid and cholesterol metabolism by the AMP-activated protein kinase.* Biochim Biophys Acta, 1992. **1123**(3): p. 231-8.

88. Hardie, D.G., et al., *Management of cellular energy by the AMP-activated protein kinase system.* FEBS Lett, 2003. **546**(1): p. 113-20.

89. Hardie, D.G., *AMP-activated/SNF1 protein kinases: conserved guardians of cellular energy.* Nat Rev Mol Cell Biol, 2007. **8**(10): p. 774-85.

90. Hadad, S.M., S. Fleming, and A.M. Thompson, *Targeting AMPK: a new therapeutic opportunity in breast cancer.* Crit Rev Oncol Hematol, 2008. **67**(1): p. 1-7.

91. Hunt, D.A., et al., *MRNA stability and overexpression of fatty acid synthase in human breast cancer cell lines.* Anticancer Res, 2007. **27**(1A): p. 27-34.

92. Bergstrom, J., et al., *Intracellular free amino acid concentration in human muscle tissue.* J Appl Physiol, 1974. **36**(6): p. 693-7.

93. Newsholme, P., et al., *Glutamine and glutamate as vital metabolites.* Braz J Med Biol Res, 2003. **36**(2): p. 153-63.

94. Kovacevic, Z. and H.P. Morris, *The role of glutamine in the oxidative metabolism of malignant cells.* Cancer Res, 1972. **32**(2): p. 326-33.

95. Eagle, H., *Nutrition needs of mammalian cells in tissue culture.* Science, 1955. **122**(3168): p. 501-14.

96. Reitzer, L.J., B.M. Wice, and D. Kennell, *Evidence that glutamine, not sugar, is the major energy source for cultured HeLa cells.* J Biol Chem, 1979. **254**(8): p. 2669-76.

97. Metallo, C.M., et al., *Reductive glutamine metabolism by IDH1 mediates lipogenesis under hypoxia.* Nature, 2011. **481**(7381): p. 380-4.

98. Anastasiou, D. and L.C. Cantley, *Breathless cancer cells get fat on glutamine.* Cell Res, 2012. **22**(3): p. 443-6.

99. Rios Garcia, M., et al., *Acetyl-CoA Carboxylase 1-Dependent Protein Acetylation Controls Breast Cancer Metastasis and Recurrence.* Cell Metab, 2017. **26**(6): p. 842-855 e5.

100. Audet-Walsh, E., et al., *The PGC-1alpha/ERRalpha Axis Represses One-Carbon Metabolism and Promotes Sensitivity to Anti-folate Therapy in Breast Cancer.* Cell Rep, 2016. **14**(4): p. 920-931.

101. McGuirk, S., et al., *PGC-1alpha supports glutamine metabolism in breast cancer.* Cancer Metab, 2013. **1**(1): p. 22.